



OPEN ACCESS

EDITED BY

Christopher C. Parrish,
Memorial University of Newfoundland,
Canada

REVIEWED BY

Sandi Orlic,
Rudjer Boskovic Institute, Croatia
Gustaaf Marinus Hallegraef,
University of Tasmania, Australia

*CORRESPONDENCE

Nicole Trefault

✉ nicole.trefault@umayor.cl

RECEIVED 03 June 2024

ACCEPTED 14 October 2024

PUBLISHED 12 November 2024

CITATION

Rodríguez-Marconi S, Krock B, Tillmann U,
Tillmann A, Voss D, Zielinski O, Vásquez M
and Trefault N (2024) Diversity of eukaryote
plankton and phycotoxins along the West
Kalaallit Nunaat (Greenland) coast.
Front. Mar. Sci. 11:1443389.
doi: 10.3389/fmars.2024.1443389

COPYRIGHT

© 2024 Rodríguez-Marconi, Krock, Tillmann,
Tillmann, Voss, Zielinski, Vásquez and Trefault.
This is an open-access article distributed under
the terms of the [Creative Commons Attribution
License \(CC BY\)](https://creativecommons.org/licenses/by/4.0/). The use, distribution or
reproduction in other forums is permitted,
provided the original author(s) and the
copyright owner(s) are credited and that the
original publication in this journal is cited, in
accordance with accepted academic
practice. No use, distribution or reproduction
is permitted which does not comply with
these terms.

Diversity of eukaryote plankton and phycotoxins along the West Kalaallit Nunaat (Greenland) coast

Susana Rodríguez-Marconi¹, Bernd Krock², Urban Tillmann²,
Anette Tillmann², Daniela Voss³, Oliver Zielinski^{3,4},
Mónica Vásquez⁵ and Nicole Trefault^{1,6,7*}

¹GEMA Center for Genomics, Ecology and Environment, Universidad Mayor, Santiago, Chile, ²Section Ecological Chemistry, Alfred Wegener Institut-Helmholtz Zentrum für Polar- und Meeresforschung, Bremerhaven, Germany, ³Institute for Chemistry and Biology of the Marine Environment, University Oldenburg, Oldenburg, Germany, ⁴Leibniz Institute for Baltic Sea Research, Warnemuende, Germany, ⁵Faculty of Biological Sciences, P. Universidad Católica de Chile, Santiago, Chile, ⁶Millenium Nucleus in Marine Agronomy of Seaweed Holobionts (MASH), Puerto Montt, Chile, ⁷FONDAP Center IDEAL- Dynamics of High Latitude Marine Ecosystem, Valdivia, Chile

The West Kallaallit Nunaat (Greenland) coast, characterized by a variety of fjords, bays, and channels influenced by glacier melting and Atlantic and Arctic waters, is one of the most affected ecosystems by climate change. Here, we combine oceanography, optics, microscopy, high throughput sequencing, microalgal strain establishments, and state-of-the-art analytical methods to fully characterize the diversity, community composition, and toxin repertoire of the eukaryotic plankton members of the coast of the West Kalaallit Nunaat (Greenland). Results indicate that the West Kalaallit Nunaat (Greenland) coast is a complex and oceanographically challenging system, where the superimposition of water masses of different origins, the penetration of light and its repercussions, generate mainly vertical, rather than horizontal heterogeneity in nutrient concentration and plankton biomass. Nevertheless, our molecular data reveal a strong homogeneity and a high diversity in the plankton community along the Greenland coast. We confirmed the presence of five phycotoxin groups: domoic acid and paralytic shellfish toxins were most abundant along the transect from Qeqertarsuup Tunua (Disko Bay) to the northern Baffin Bay, while spirolides, yessotoxins and pectenotoxins were predominant in Nuup Kangerlua (GodthaabFjord) and Qeqertarsuup Tunua (Disko Bay). Concentrations of these phycotoxins correlate differently to temperature, salinity and nutrients, reflecting the ecological differences of their producers. Patterns of paralytic shellfish and spirolide toxins suggest the presence of genetically distinct populations of *Alexandrium* along the Western Kalaallit Nunaat (Greenland). Phytoplankton strains isolated during this

oceanographic campaign resemble, in most cases, the toxin profiles of the respective field stations. Overall, this work shows the diversity and community composition of the plankton at the Western Kalaallit Nunaat coast and reveals a distinct spatial distribution of phycotoxins, with certain toxin groups restricted to specific areas.

KEYWORDS

Arctic, 18S rRNA gene, high throughput sequencing, plankton diversity, phycotoxin profiles, climate change, harmful algal blooms, Fjord ecosystems

1 Introduction

In the past 150 years, the Arctic has experienced a two to three times higher temperature increase than the average global temperature increase (Wassmann, 2011). This temperature increase leads to a decreasing ice cover and increasing solar irradiance, which is expected to influence the survival, life cycles, and growth of a variety of eukaryotic plankton species (Arrigo et al., 2017), including those that generate harmful algal blooms (HAB) associated with toxin production. There is increasing evidence that HAB are growing both in frequency and extension worldwide, with fjords and enclosed marine areas experiencing notorious effects and a broad spectrum of impacts on human activities and the welfare of marine ecosystems (Berdalet et al., 2015; Gobler, 2020; Hallegraef et al., 2021).

Fjord and bay systems in the Arctic are complex and dynamic marine areas where geographic, atmospheric, and hydrographic factors closely interact (Rysgaard et al., 2003). Specifically, the fjords, bays, and channels of Kalaallit Nunaat (Greenland) are characterized by shallow sills and a strong influence of oceanic waters from the Atlantic and Arctic waters on the continental shelves (Straneo and Cenedese, 2015). Besides, their numerous glaciers, which can be land- or marine-terminating, determine unique environments with high productivity due to glacier runoff and recurrent intrusions of freshwater and nutrients (Meire et al., 2023). These systems are prone areas for HAB; nevertheless, there is limited knowledge about the diversity of microbial plankton, including those able to produce toxins and harmful effects over this threatened ecosystem. Understanding plankton compositional patterns along the Kalaallit Nunaat (Greenland) coast, including their fjords, bays, and channels, will undoubtedly increase our forecasting capacity to see the effects of climate change related to marine toxins.

Marine toxins are produced by several microbial members of the eukaryotic plankton and can be broadly classified as hydrophilic toxins, including paralytic shellfish toxins (PSTs) and domoic acid (DA), and lipophilic toxins, which include okadaic acid (OA), dinophysistoxins (DTXs), pectenotoxins (PTXs), yessotoxins (YTXs), gymnodimines (GYMs), azaspiracids (AZAs), and spirolides (SPXs). In the Kalaallit Nunaat (Greenland) coast,

PSTs, DA, SPXs and YTXs have been detected, and many of their producers have been identified and isolated (Hansen et al., 2011; Baggesen et al., 2012; Tillmann et al., 2014; Richlen et al., 2016; Salazar-Pérez et al., 2016; Elferink et al., 2017; Bruhn et al., 2021). A seasonal survey of toxins and their producers at Qeqertarsuup Tunua (Disko Bay), a large bay on the western coast of Greenland that constitutes a wide southeastern inlet of Baffin Bay, showed that dissolved toxins followed the succession pattern of the particulate fraction with a delay in time (Bruhn et al., 2021), allocating importance to constant monitoring phycotoxins along the Kalaallit Nunaat (Greenland) coast.

Diversity and microbial dynamics in freshwater-influenced coastal systems at high latitudes are significantly affected by seasonality. This influence has been widely studied in Kalaallit Nunaat (Greenland), Chukchi and Beaufort Seas (Sukhanova et al., 2009), the Fram Strait (Wietz et al., 2021), and the fjords of Norway (Marquardt et al., 2016). Seasonal patterns of microbial eukaryote succession along the Kalaallit Nunaat coast have been also observed, typically characterized by a spring bloom from April to May, followed by a period of reduced activity or interbloom period and a subsequent dinoflagellate bloom (Juul-Pedersen et al., 2015; Krawczyk et al., 2015; Arrigo et al., 2017). Historically, research on plankton diversity in this area has focused primarily on larger eukaryotes (>20 µm), particularly diatoms, identified by light microscopy. This approach has highlighted *Thalassiosira*, *Fragilariopsis*, and *Chaetoceros* as the predominant genera in this region, each associated with specific physicochemical conditions in the water column (Krawczyk et al., 2014). However, because light microscopy is often insufficient for accurately capturing the full diversity of smaller phytoplankton, our understanding of the community composition in the Kalaallit Nunaat (Greenland) coast and its links to toxin production and oceanographic conditions remains incomplete.

Previous assessments of protist diversity using molecular analyses based on high throughput sequencing -or tag sequencing- have shown an unexpected stability within the rare biosphere, indicating a potential constant protist reservoir and dominance of Syndiniales, *Micromonas* and *Phaeocystis* within the abundant biosphere in the central Arctic Ocean (Kilias et al., 2014). These findings were subsequently confirmed in Fram Strait

and large parts of the Central Arctic Ocean (Nansen Basin, Amundsen Basin), where it was observed that picoplankton accounted for most of the chlorophyll-a biomass in this area (Metfies et al., 2016). At Qeqertarsuup Tunua (Disko Bay) and Vaigat Strait, a strait that separates Nuussuaq Peninsula in the northeast from Qeqertarsuaq (Disko) Island in the southwest, tag sequencing of different plankton size-fractions during the late summer revealed that the diversity and the effect of environmental parameters varied both within and among size-fractions (Elferink et al., 2017). Finally, the combination of tag sequencing and metatranscriptomic analysis of microeukaryotes within coastal surface waters of West Greenland and regions from ice-free Northwest Iceland revealed that changes in temperature and salinity were more closely correlated with metabolic functions and community composition (Elferink et al., 2020).

Altogether, these findings show a higher diversity within the pico- and nanoplankton fraction, which are precisely the size fractions that are less accessible through microscopy techniques. However, most of these studies have been restricted to specific areas or specific size fractions, limiting a comprehensive assessment of marine microbial eukaryotes across the entire coast of Greenland. To our knowledge, there are currently no studies that thoroughly address all plankton size fractions, using both tag sequencing and microscopy, along with chemical approaches to accurately identify toxins and the isolation of toxin-producing plankton strains in West Greenland.

During the boreal summer of 2017, and thanks to the GreenHAB II (MSM65) cruise onboard the R/V Maria S. Merian, we comprehensively characterized the microbial eukaryotic

plankton along the West Kalaallit Nunaat (Greenland) coast between 64° and 75°N, including the Nuup Kangerlua (Godthaab Fjord) -the longest fjord on the Labrador Sea- and the Qeqertarsuup Tunua (Disko Bay). The specific aims of this study were: 1) To integrate different approaches and analyses to characterize the diversity, community composition and distribution of microbial eukaryotic plankton in the unique area of the West Kalaallit Nunaat (Greenland) coast. 2) Analyze the presence and distribution of toxins and toxin producers by combining high throughput sequencing, microscopy, strain establishment, and state-of-the-art analytical techniques. 3) Characterize the link between plankton community composition and the oceanographic conditions in this area, focusing on toxin-producing plankton species.

2 Materials and methods

2.1 Study site, sampling, and hydrographic observations

Data were collected during the MSM65 cruise from St. John's, Canada, to Nuuk, Kalaallit Nunaat (Greenland), between June 25th and July 19th, 2017, aboard the R/V Maria S. Merian. Besides station 1 at the Labrador Sea, the remaining 49 sampling stations were grouped into three areas: Nuup Kangerlua (Godthaab Fjord) (area A: 13 stations), transect (area T: 14 stations), and Qeqertarsuup Tunua (Disko Bay) (area B: 22 stations) (Figure 1). Nuup Kangerlua (Godthaab Fjord (64°N) is the most extensive fjord system in southwest Kalaallit Nunaat (Greenland), connected to the

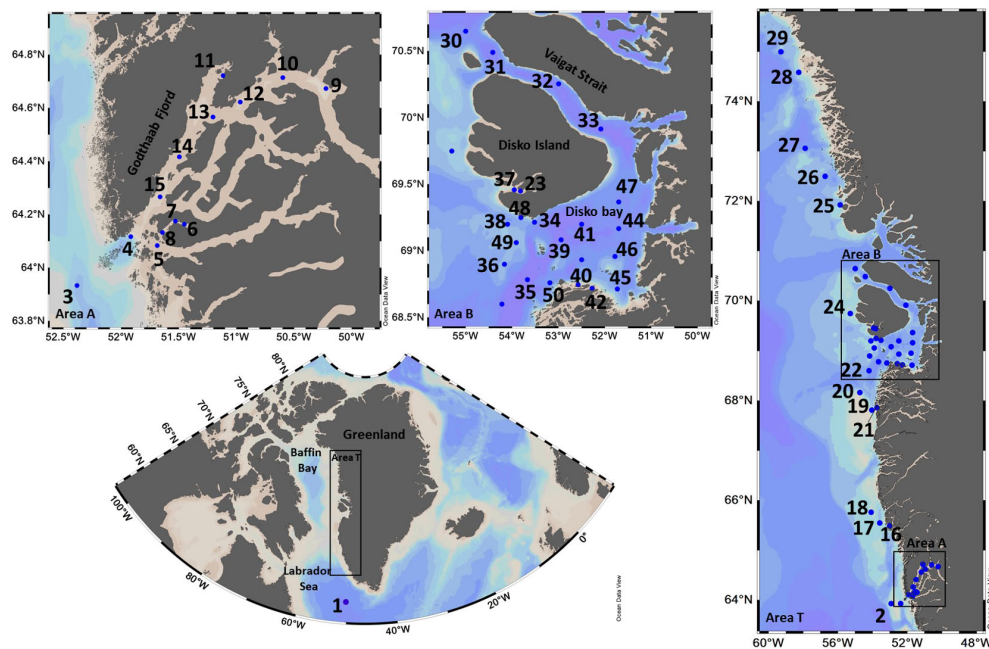


FIGURE 1

Map of the Arctic and West Kalaallit Nunaat (Greenland) showing the study areas during the MSM65 cruise aboard the R/V Maria S. Merian in 2017. The sampling stations are indicated by blue circles and labeled with numbers. Area T represents the coastal transect with 14 sampling stations, area A corresponds to the Nuup Kangerlua (Godthaab Fjord) with 13 stations, and area B encompasses Qeqertarsuup Tunua (Disko Bay) with 22 stations. The color gradient illustrates different contour lines of water depth.

Kalaallit Nunaat (Greenland) Ice-Sheet (Mortensen et al., 2011). Qeqertarsuup Tunua (Disko Bay (70°N) is located at the border of the high and low Arctic zone part. It is highly influenced by glacier melting, which generates differences in salinity and temperatures between the inner and outer bay (Heide-Jørgensen et al., 2007).

At each station, the CTD system used was an SBE 911plus probe (Sea-Bird Scientific Inc). It was attached to a SBE 32 Carousel Water Sampler containing 24 x 20-liter Ocean Test Equipment Inc. bottles. The system was equipped with double temperature (SBE 3) and conductivity sensors (SBE 4), a pressure sensor (Digiquartz), an oxygen Optode (Aanderaa Optode 4831F), an altimeter (Benthos), and a chlorophyll fluorometer combined with a turbidity sensor (WET Labs ECO_AFL FL). The sensors were pre-calibrated by the manufacturers. Data were recorded with the Seasave V 7.23.2 software and processed using the Sea-Bird SBE Data Processing. The ship position was derived from the shipboard GPS linked to the CTD data. Salinity was quality checked by reference samples [n=42], measured with an Optimare Precision Salinometer (OPS S/N 003) four months after the cruise (S1: R² 0.9997, S2: R² 0.9997).

2.2 Aquatic optics

A HyperPro II profiling system (SeaBird Scientific Inc, former Satlantic) was used to collect hyperspectral underwater light field data in free-falling mode. The system consists of one hyperspectral irradiance and one hyperspectral radiance sensor. A second hyperspectral irradiance sensor was mounted on the research vessel to match above-water irradiance reference measurements. Profiles were conducted at each station depending on sea and weather conditions. To avoid ship shadow, the profiler was deployed at about 50 m away from the ship. All sensors were pre-calibrated by the manufacturer. Data were recorded with the SatView software (V 2.9.5_7) and pre-processed from raw to Level 3a using the ProSoft Processing software (V 7.7.19_2). Measured data were binned in 1 m depth intervals. A dark correction was made automatically based on shutter measurements by the instrument. Post-processing was made following (Mueller et al., 2003; Organelli et al., 2016). The 1% PAR depth was determined to compare the penetration depth for each station.

2.3 Onboard sample processing

At each station, 5 L water samples were taken at different photic zone depths. Samples were grouped into four categories: 2-5 m, hereafter referred to as surface (S); 10-20 m, hereafter referred to as above Deep Chlorophyll Maximum (aDCM); 10-40 m, hereafter referred to as Deep Chlorophyll Maximum (DCM); and 40-60 m, hereafter referred to as below Deep Chlorophyll Maximum (bDCM). The depth ranges for each category refer to variable depths depending on the sampling station (for more details, please see [Supplementary Table S1](#)).

Subsamples were size-fractionated through 0.2 (GSWP), 3 (SSWP), and 20 (NY20) μm diameter pore Millipore filters using Swinnex holder systems (47 mm) and a Cole Parmer 1-100 rpm peristaltic pump. Plankton samples were taken at every sampling

station by vertical 20 μm net tows of the upper 30 m water column. Subsamples were fixed with Paraformaldehyde for later detailed microscopy analysis. Flow cytometry samples (1.5 mL) were fixed in triplicate using Glutaraldehyde (0.25% final concentration) for general microbial abundance counting. Samples were fixed for 20 min at RT, flash-frozen in liquid nitrogen, and stored at -80°C until further analysis.

For nutrient analyses, unfiltered water (nitrate, nitrite, ammonium, phosphate, and silicate) was collected in 50 mL LDPE bottles and analyzed as described in (Graeve et al., 2018). To determine chlorophyll-a (Chl-a) concentration, up to 3 L water was sampled and filtered on glass fiber filters (47 mm diameter, pore size approx. 0.7 μm; Whatman, UK), pre-washed and rinsed with 0.2 μm filtered seawater. The filters were subsequently frozen and stored at -80°C on board and were analyzed in the laboratory after the cruise. Pigment extraction was done in 90% acetone-water solution with an overnight incubation at 4°C. Extracts were centrifuged, and the fluorescence of the supernatant was determined at 665 nm using a pre-calibrated TD-700 laboratory fluorometer (Turner Designs, San Jose, USA). Chl-a concentration was calculated according to EPA method 445 (Arar and Collins, 1997). Nutrient data is available with open access: <https://doi.org/10.1594/PANGAEA.887413>.

2.4 Flow cytometry

Cell abundances of total bacteria, photosynthetic picoeukaryotes, photosynthetic nanoeukaryotes, and Cryptophytes were determined using an Accuri C6 Plus (Becton Dickinson). Light scatter and fluorescence were normalized by adding 1 and 3 μm fluorescent beads. For quantification of bacteria, Sybr Green I was used, and counts were based on side scatter and green fluorescence (530/40 nm). To identify the phytoplankton groups, we used the 488 nm excitation laser. We collected the fluorescence at 580/15 nm (orange fluorescence) as a proxy for phycoerythrin and 670/LP (red fluorescence) as a proxy for chlorophyll, according to Marie et al., 2005.

Bacterial biomass was calculated assuming that one bacterial cell contains 20 fg C (Lee and Fuhrman, 1987). Biovolumes were calculated based on flow cytometry counts. A calibration curve was constructed using FSC values from 1, 2, 3, and 6 μm beads as follows:

$$\text{Diameter} = 1,2325 \ln(\text{FSC}) - 11,642 \quad (1)$$

Assuming cells were spherical, biovolumes were converted into a mean carbon cellular quota (QC, calc) according to the QC, calc = a * Biovolume^b relationship and using conversion factors a and b reported by Menden-Deuer and Lessard, 2000, with a= 0.32, 0.27 and 0.25 for picophytoplankton, nanophytoplankton and cryptophytes, respectively and b = 0.86.

2.5 DNA extraction

Filters were thawed, and half of the filters were cut into 1 mm² pieces and incubated in lysis buffer (TE 1x/NaCl 0.15 M) with 10% SDS and 20 mg mL⁻¹ proteinase K at 37°C for 1 h. DNA was

extracted using 5 M NaCl and hexadecyl-trimethyl-ammonium bromide (CTAB) extraction buffer (10% CTAB, 0.7% NaCl), which was incubated at 65°C for 10 min before protein removal using a conventional phenol-chloroform method. DNA was precipitated using ethanol at -20°C for 1 h and resuspended in 50 µL deionized water (Milli-Q, Millipore). DNA integrity was evaluated by agarose gel electrophoresis and quantified using a fluorometric assay (Qubit 2.0 fluorometer).

2.6 Amplicon sequencing and bioinformatic analyses

The 18S rRNA gene was amplified and sequenced using the eukaryote-specific primers E572F (CYGCGGTAATTCAGCTC) and E1009R (AYGGTATCTRATCRTCCTTYG) that target the hypervariable region V4 (Comeau et al., 2011). Illumina amplicon sequencing was performed at the Integrated Microbiome Resource (IMR, Halifax, Canada) using the Miseq technology. Sequencing succeeded in 377 out of 576 samples due to low concentrations of the genetic material, mainly in microplanktonic samples (20–200 µm).

Sequence data were processed using the R package DADA2 (Callahan et al., 2017) in R version 3.4.4. (R Core Team, 2018) Sequences were pre-filtered to remove ambiguous bases before primer removal. Primers were removed using cutadapt tool (version 1.10) (Martin, 2011). Quality filtering of the reads was performed using filterandtrim function with maxN = 0, maxEE = c(10,10), truncLen = c(260, 220), truncQ = 2, minLen = c(260, 220). After unique sequences were generated, forward and reverse were merged, and Amplicon Sequence Variants (ASVs) were generated. Chimeras were removed from the sequences, and taxonomic assignments were performed with the PR2 database (v4.12.0) (Guillou et al., 2013). ASVs assigned to Embriophyceae and Metazoa and those composed of less than 50 reads across the whole dataset were removed before further analyses. Unclassified Dinophyceae ASVs were manually inspected by BLASTn against the NCBI nr database (November 2023) (Sayers et al., 2022).

2.7 Microscopy of plankton samples

Plankton net tow samples were inspected and documented for microplankton community composition and potentially toxic species on board using an inverted microscope (Axioskop 35, Zeiss) equipped with an HD digital camera (Gryphax Jenoptik). In addition, Niskin bottle samples were used to qualitatively check the nanoplankton community for the presence of small and potentially toxic species. For this, 1 L sample pooled from three depth categories (S, aDCM, and DCM) was gently concentrated using 5 µm pore size polycarbonate filters and observed using the inverted microscope.

For quantitative micro- and nanoplankton plankton analysis, Niskin bottle water samples from three depths (S, aDCM, and DCM) were pooled, and 200 mL were fixed with Lugol (2% final concentration). From these samples, 50 mL each from 38 selected

stations (see Supplementary Table S1) were concentrated in sedimentation chambers and counted using an inverted microscope (Axioskop 35, Zeiss). Cells were identified to species level or assigned to counting categories at higher taxonomic levels. Species or groups were subdivided into different size categories where necessary. For each counting unit, cell densities were transformed to carbon biomass by size- and shape-specific conversion factors as provided by the Baltic Marine Environment Protection Commission (HELCOM) via https://www.ices.dk/data/Documents/ENV/PEG_BVOL.zip.

For a direct comparison of toxin data and abundance of toxigenic dinophyte species (i.e., *Alexandrium* spp., *Dinophysis acuminata*, *D. acuta*, *D. norvegica*, *Protoceratium reticulatum*), 1 mL of Paraformaldehyde fixed net-tow samples from 33 selected stations were stained with a drop of Calcofluor-white, settled in a small sediment chamber, and analyzed at 200–640 x magnification with an Axiovert 200 (Zeiss) epifluorescence inverted microscope and UV excitation. Cells of *Alexandrium* spp. were identified and counted based on cell shape and plate details but were not quantitatively determined at the species level.

2.8 Isolation and characterization of microalgal strains

Single cells of potentially toxigenic dinoflagellates were isolated on board from live net tow concentrates under a stereomicroscope (M5A, Wild) by micropipetting. Single cells were transferred into individual wells of 96-well tissue culture plates (Techno Plastic Products) containing 250 µL of medium prepared from 0.2 µm sterile-filtered medium (Keller et al., 1987) diluted with seawater from the sampling location at a ratio of 1:10. The original K-medium receipt was slightly modified by replacing the organic phosphorus source by 3.62 µM Na₂HPO₄. Plates were incubated at 10°C in a controlled environment growth chamber (Model MIR 252, Sanyo Biomedical). Unialgal isolates were transferred to 24-well tissue culture plates, each well containing 2 mL medium. Exponentially growing isolates were finally used as inoculum for batch cultures in 65 mL polystyrene cell culture flasks and were maintained after that at 10°C under a photon flux density of 30–50 µmol m⁻² s⁻¹ and a 16:8 h light: dark photoperiod in a temperature-controlled walk-in growth chamber. All strains were sampled for morphological and toxigenic characterization as described in Tillmann et al., 2014. For the determination of thecal plate pattern of selected strains, Lugol-fixed subsamples were stained with Solophenyl Flavine (Carbosynth) and inspected with epifluorescence microscopy.

Species identification was confirmed for some selected strains by LSU and ITS rRNA gene sequencing as described in Tillmann et al. (2017). For this, the PCR amplicons were purified using the NucleoSpin Gel and PCR clean-up kit (Macherey-Nagel) and sequenced directly in both directions on an ABI PRISM 3730XL (Applied Biosystems by Thermo Fisher Scientific) as described in (Tillmann et al., 2017). Raw sequence data were processed using the CLC Genomics Workbench 12 (Qiagen, Hilden, Germany). Molecular identification of *Alexandrium catenella*

was based on the positive signal of DNA tested by qPCR using primers specifically designed to detect *A. catenella* (Toebe et al., 2013), including three strains of *A. catenella* and *A. tamutum* from the AWI culture collection as positive and negative control, respectively.

2.9 Phycotoxin detection

The cell pellets from the plankton net tows and monoclonal cultures were harvested by centrifugation, suspended in 500 μ L methanol for lipophilic toxins or 0.03 M acetic acid for hydrophilic toxins, and subsequently extracted by homogenization, filtered and measured by liquid chromatography with post-column derivatization and fluorescence detection (LC-FLD) for hydrophilic PSTs and by liquid chromatography coupled to tandem mass spectrometry (LC-MS/MS) for all other analyzed toxin groups.

2.10 Liquid chromatography with post-column derivatization and fluorescence detection

The aqueous extracts were separated by reverse-phase ion-pair liquid chromatography following minor modifications of previously published methods (Diener et al., 2007; Krock et al., 2007). The LC-FLD analysis was conducted on an LC1100 series liquid chromatography system equipped with a Phenomenex Luna C18 reversed-phase column (250 mm X 4.6 mm id, 5 μ m pore size) pre-column. The column was coupled to a PCX 2500 post-column derivatization system. The injection volume was 20 μ L, and the autosampler was cooled to 4°C. The eluate from the column was oxidized with periodic acid before entering the 50°C reaction coil, after which it was acidified with nitric acid. The toxins were detected by dual-monochromator fluorescence (λ_{ex} 333 nm; λ_{em} 395 nm) (Van de Waal et al., 2015).

2.11 Lipophilic toxin measurement of field samples by LC-MS/MS

Mass spectral experiments were performed on a triple quadrupole mass spectrometer coupled to an Agilent model 1100 LC. After injection of 5 μ L of the sample, lipophilic toxins were separated by reversed-phase chromatography on a C8 phase, and gradient elution was performed with water and acetonitrile. The chromatographic run was divided into three periods: one for DA, one for GYMs and SPXs, and one for OA, DTXs, PTXs, YTXs, and AZAs. Selected reaction monitoring (SRM) experiments were carried out in positive ion mode (Krock et al., 2013). In addition, specific SRM experiments were performed for the toxin classes of AZAs (Krock et al., 2019), YTXs (Sala-Pérez et al., 2016), and cycloimines, including SPXs and GYMs (Nieva et al., 2020).

2.12 Statistical analyses

Phylogenetic diversity (PD) was calculated using the library Picante (Kembel et al., 2010) in R environment (R Core Team, 2022). Shannon index (H') was calculated using the software Primer-e version 6. Graphs were constructed with GraphPad Prism v8. nMDS were made based on sequence number using the vegan package (Oksanen et al., 2022) in R environment using the Hellinger transformation and the Bray-Curtis distance measure. A comparison of high throughput sequence data with microscopy data from toxin producers was made by summing up reads from S, aDCM, and DCM depths. Spearman correlations were conducted with these data, toxin amounts, and cell abundances of toxins producers using GraphPad Prism v8. Stations and gridded maps were generated using Ocean Data View (version 5.3.0) (Schlitzer, 2022).

Paired tests for nutrients, cell abundance, diversity, and Chl-a were performed in the software Past3 (Hammer et al., 2001). The normality test applied was Shapiro-Wilk (Shapiro and Wilk, 1965). When distribution was normal, ANOVA and Tukey test were applied. Otherwise, Kruskal-Wallis and Mann-Witney tests were used to compare diversity measures between size fractions and depth categories in each area. Kolmogorov-Smirnov two-sample test was applied to explore differences between depth categories when data distribution was non-normal.

3 Results

3.1 Oceanographic context

During June-July 2017, we sampled 49 stations located along the West Coast of Kalaallit Nunaat (Greenland) within the photic zone of the water column. These sampling stations were grouped into three areas based on their oceanographic conditions: Nuup Kangerlua (Godthaab Fjord) (area A), a coastal transect (area T), and Qeqertarsuup Tunua (Disko Bay)-Sullorsuaq (Vaigat) Strait (area B) (Figure 1).

Seawater temperature showed significant stratification at stations with freshwater input in areas A and B. Most stations recorded a salinity of nearly 34, except at the head of area A, where surface salinity decreased to 22.8 due to freshwater input from glacier discharge, and in area B where salinity values were around 32. In contrast, area T showed more stable distribution of temperature and salinity (Supplementary Figure S1).

The depth of the photosynthetically active radiation (PAR) at 1% intensity varied from ~ 20 to 40 m across the study area. Light penetration was greatest at the mouth of Nuup Kangerlua (Gothaab Fjord) and at the Sermeq Kujalleq (Jacobshavn Isbraer) outlet (near Station 44), reaching depths of around 40 meters. Unlike area T, light penetration was heterogeneous across the region (Supplementary Figure S2).

Nutrients were mainly depleted at the surface, except at the head of the Nuup Kangerlua (Godthaab Fjord) (area A) (Supplementary Figure S1). Nitrate was lower at the surface compared to the DCM in the three study areas (Kolmogorov-Smirnov between depth categories

area A: $D=0.78$, $p=0.002$; area T: $D=0.85$, $p<0.001$; and area B: $D=0.95$, $p<0.001$). Phosphate concentration was higher at the surface compared to DCM, only in areas A (ANOVA $F=16.6$; $p<0.001$) and B (Kruskal-Wallis $H=9.9$, $p=0.007$). Chl-*a* ranged from 0.1 to 3.95 mg m^{-3} (Figure 2A), and displayed depth-differentiation only in area B, revealing significant differences between surface and DCM concentrations (Kolmogorov-Smirnov test, $D=0.6$, $p=0.0007$). The highest concentrations coincided with lower PAR 1% depths, suggesting that glacier melt water influenced Chl-*a* levels.

3.2 Microbial abundances and biomass

Flow cytometry (FCM) measurements indicated that the abundance of bacterial and photosynthetic picoeukaryotes showed

depth differentiation between bDCM and the other depth categories. Bacterial biomass as determined by FCM counts ranged from 4.7 to $52.8 \text{ } \mu\text{g C L}^{-1}$. In comparison, picophytoplanktonic biomass ranged from 0.005 to $24.2 \text{ } \mu\text{g C L}^{-1}$, being significantly lower at the bDCM than at the upper depths (Kruskal-Wallis $H=46.2$, $p=5e-10$). Nanophytoplankton biomass, which varied from 0.26 to $37.5 \text{ } \mu\text{g C L}^{-1}$, also showed significantly lower values at DCM (Kruskal-Wallis $\chi^2=15.9$, $p=0.001$). Conversely, Cryptophyte biomass ranged from 0.06 to $155 \text{ } \mu\text{g C L}^{-1}$ and was significantly higher at DCM (Kruskal-Wallis $\chi^2=11$, $p=0.01$). Picoplanktonic biomass was lower at area T (Figure 2A).

The total biomass of the plankton community, as assessed by fixed sample microscopy, ranged from 39 to $1077 \text{ } \mu\text{g C L}^{-1}$ (Figure 2B). The highest biomass consisted primarily of diatoms and other flagellates (excluding dinoflagellates) with no differences

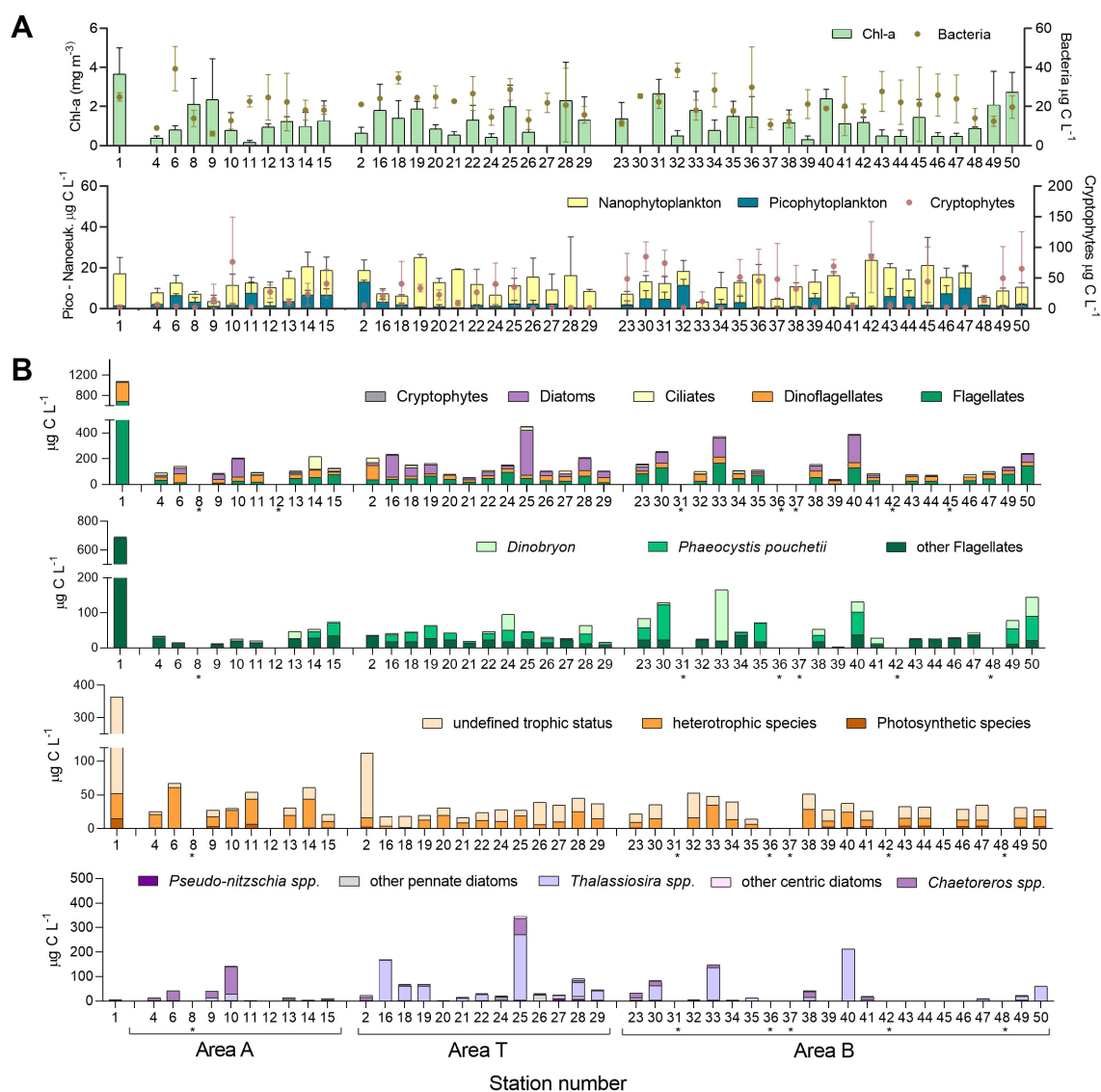


FIGURE 2

Microbial biomass from surface to the Deep Chlorophyll Maximum. (A) Chlorophyll-*a* (Chl-*a*) concentrations, estimated by fluorometry measurements, as a proxy of phytoplankton biomass. Microbial biomass estimates derived from flow cytometry including counts for photosynthetic pico- and nanoeukaryotes, Cryptophytes, and Bacteria. (B) Estimated biomass of microbial eukaryotes $>5 \text{ } \mu\text{m}$ based on microscopy counts from pooled abundances from surface to DCM. Stations marked with an asterisk * indicate missing microscopy data.

in biomass distribution across the three subareas (Figure 2B). The Haptophyte *Phaeocystis pouchetii* was the most abundant species with abundances above 10^6 cell L^{-1} , mainly in area B (Supplementary Figure S3B). The Chrysophyte *Dinobryon balticum* peaked in area B (Supplementary Figure S3C). Among the dinoflagellates, biomass contribution of species known to have plastids (photosynthetic species) was low (Supplementary Figure S3D), while species known to be heterotrophic were relatively abundant (Supplementary Figure S3E). However, for a considerable proportion of dinoflagellate counts - mainly small naked and thecate specimens - species identification was not possible, leaving their trophic status undefined. Diatom biomass was dominated by species of *Pseudo-nitzschia*, *Thalassiosira*, and *Chaetoceros*. The latter genus (with *C. debilis* and *C. socialis* as the most abundant species) displayed high abundances at stations 6, 9, and 10 in area A and station 25 in area T (Supplementary Figures S3I, J). Dense populations of *Thalassiosira* spp. were mainly present in area T and at some stations of area B (Supplementary Figure S3H). Chain-forming pennate diatoms (*Fragillaria* spp. and similar species) were found in higher abundance at the northernmost stations in area T (Figure 2B, Supplementary Figure S3H). Additionally, onboard light microscopy of living samples revealed the presence of several species of potentially toxic plankton genera (Supplementary Figure S3). Species of the diatom *Pseudo-nitzschia* (Supplementary Figures S4E, F) were abundant and widespread, but species identification using light microscopy was impossible. At least three species of *Dinophysis* were identified, *D. acuta*, *D. accuminata*, and *D. norvegica* (Supplementary Figures S4G–J). A fourth and significantly smaller and scarce species (Supplementary Figure S4K) was not identified at the species level. Within *Alexandrium*, a few cells of *A. ostenfeldii* could be identified by LM through the presence of the characteristically large ventral pore (Supplementary Figure S4T). In contrast, other *Alexandrium* species could only be retrospectively identified by using thecal plate staining and sequence analyses of isolated strains.

3.3 Phylogenetic distribution, diversity, and community composition of microbial eukaryotic plankton

The tag-sequencing dataset yielded approximately 15 million reads clustered into 4,674 Amplicon Sequence Variants (ASVs). Of these, only 1,415 ASVs (30%) had more than 50 reads, collectively accounting for 99.7% of total reads, indicating that most of the microbial eukaryote communities belong to the rare biosphere.

ASVs were classified into ten known eukaryotic taxonomic divisions using the PR2 database classification scheme (Figure 3A). Among 23 dominant eukaryotic classes (>1% at least in one station), fourteen were ubiquitous across the 46 stations for which high throughput sequencing was performed (Figure 3B). Within Dinoflagellata, the classes with the most ASVs were Dinophyceae (358 ASVs) and Syndiniales (193 ASVs) (Figure 3C). Dinophyceae was also the class with the highest read number across the whole dataset (Figure 3D). The proportion of reads for each taxonomic group agreed with expected organism

sizes, with Mamiellophyceae, Picozoa, and Chlorarachniophyceae were enriched in the 0.2–3 μm size fraction. Most classes were present in the 3–20 μm size fraction, whereas the 20–200 μm size fraction showed an enrichment of Bacillariophyta, Cercozoa, and Ciliophora (Figure 3E). The majority of reads from major eukaryotic lineages were found at bDCM, except for Chlorarachniophyceae (more abundant at the surface), and Pelagophyceae, Cryptomycota, and Chytridiomycota (most abundant at DCM) (Figure 3F).

To assess potential phycotoxin producers, dinoflagellates and other plankton groups were analyzed separately. Faith's Phylogenetic Diversity (PD) and Shannon diversity (H') indices were significantly higher for non-dinoflagellate groups in area A, while only PD was significantly higher for dinoflagellates in area B. Diversity within Dinoflagellata varied among size fractions across the three study areas and water depths, Supplementary Table S2).

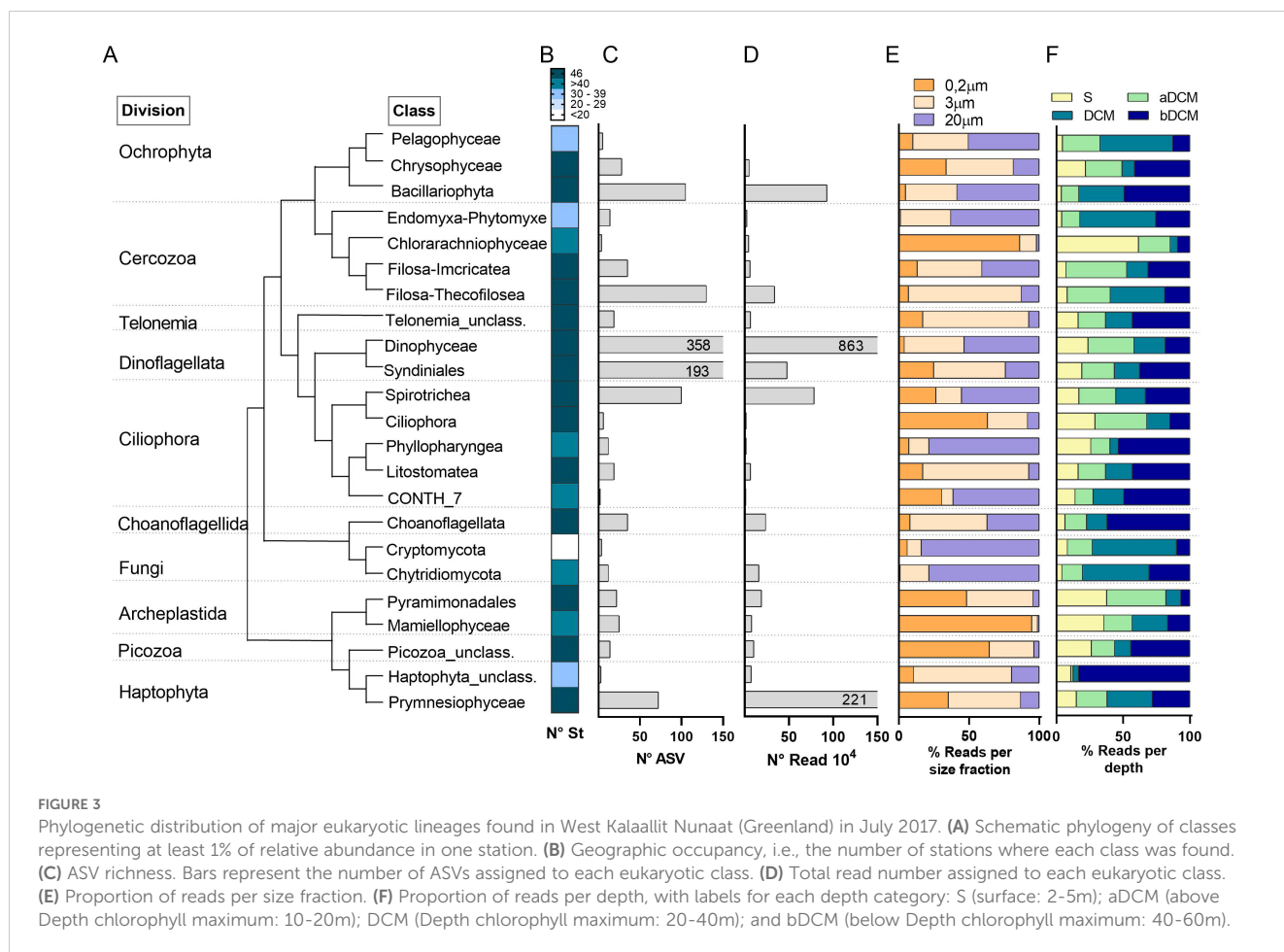
Except for dinoflagellates, eukaryotic plankton community composition along the West Kalaallit Nunaat (Greenland) coast was dominated by Haptophyta and Ochrophyta, particularly *Phaeocystis* (Prymnesiophyceae), and *Chaetoceros* (Bacillariophyta) (Figure 4). Unclassified Ciliophora and Mamiellophyceae were also significant, especially in area T and outer stations of areas A and B. Area A displayed the highest relative abundance of Prymnesiophyceae (primarily *Phaeocystis*), while area T had more of heterotrophic classes such as Spirotrichea and Filosa-Thecofilosea and a higher proportion of Chlorophyta. Bacillariophyta decreased markedly at the northernmost stations, but occurred in higher abundances in Qeqertarsuup Tunua (Disko Bay, area B) and Sullorsuaq (Vaigat Strait) (Figure 4). *Gyrodinium* was the dominant dinoflagellate, averaging 76%, 78%, and 58% relative abundance in areas A, T, and B, respectively, while Syndiniales were mainly represented by Dino-Group II clade 1 (average 6% among the three areas) (Figure 4).

Non-metrical dimensional scaling (nMDS) analyses revealed that the community composition of microbial eukaryotes was homogenous throughout the photic zone (Supplementary Figure S5, Supplementary Table S3). ANOSIM values indicated high homogeneity across the study area for all microbial eukaryotes (R ranges: 0.11 – 0.25), suggesting that depth does not affect overall community composition within the photic zone.

3.4 Distribution of phycotoxin and their producers

The phycotoxins detected in plankton samples were spirolides (SPXs), pectenotoxin-2 (PTX-2), paralytic shellfish toxins (PSTs), domoic acid (DA), and, to a lesser extent, yessotoxins (YTXs). Toxin abundances varied among stations, exhibiting a spatial distribution (Figure 5). DA and PSTs were most abundant in area T, while SPXs, YTXs, and PTX-2 were predominant in areas A and B (Supplementary Figure S6). DA exhibited the highest concentrations north of the study area (Supplementary Figure S6).

The PST profiles varied between inner water bodies (areas A and B) and open coastal water (area T). Areas A and B contained only saxitoxin (STX) and gonyautoxins-2/3 (GTX-2/3), whereas toxin profiles of area T were dominated by the *N*-hydroxy variants



neosaxitoxin (NEO) and gonyautoxins-1/4 (GTX-1/4). The only exception was station 23, located in the inner Kangerluk (Disko Fjord), which exhibited a unique PST profile with mainly NEO and minor contributions of STX and GTX-2/3 (Figure 5A).

The SPX profiles were relatively diverse, with nine SPX variants. In area A, SPX profiles were dominated by SPX C, 20-methyl SPX G, and a not fully characterized SPX provisionally named SPX-696/2. In contrast, SPX profiles of area B were dominated by SPX A, 20-methyl SPX G, and a not fully characterized SPX named SPX-720 (Figure 5B). The only known SPX-producer, *A. ostenfeldii*, was detected at most stations though it accounted for only 0.6% of the total Dinoflagellata reads. *Alexandrium* spp. were identified in 27 out of 33 stations by microscopy (Supplementary Table S4).

PTX-2 was detected at 11 stations within Qeqrtarsuup Tunua (Disko Bay) and Nuup Kangerlua (Godthaab Fjord) with the highest abundance at station 11 (Supplementary Figure S6), which also displayed the highest cell abundance of *Dinophysis*, with dominance of *D. acuminata*, lower abundances of *D. norvegica* and rare occurrence of *D. acuta*.

YTXs were predominantly in open oceanic waters along the Kalaallit Nunaat (Greenland) West coast. Most YTX profiles consisted of YTX, YTX-1131 (corresponding to entry #81 in Miles et al. (2005), and carboxy-YTX. However, along transect North and in Sullorsuaq (Vaigat) Strait, YTX abundances were

lower and mainly comprised YTX-991 [entries #4, #5, and/or #6 in Miles et al. (2005)] (Figure 5C). *Protoceratium reticulatum*, a known YTX producer, was found mainly in areas A and B, with a high correlation between its abundance in net tows and YTX content (R^2 0.85) (Supplementary Table S4).

Within the phycotoxins detected, SPXs, PTX-2, PSTs, DA, and YTXs, we found significant and positive correlations between toxin concentrations and different environmental parameters. Positive correlations were found between SPX and temperature (R : 0.63, $p > 0.01$), PTX-2 and silicic acid (R : 0.8, $p < 0.01$) and turbidity (R : 0.63, p : 0.02) and YTX also with temperature (R : 0.55, p : 0.01). On the other hand, SPXs showed negative correlation with salinity (R : -0.41, $p < 0.01$) and silicic acid (R : -0.45, $p < 0.01$). STX exhibited weak but negative correlations with nutrients (nitrate R : -0.43, $p < 0.05$; silicic acid R : -0.28, $p < 0.05$; phosphate R : -0.26, $p < 0.05$).

3.5 Isolated strains of potentially toxic species

Among many microalgae strains isolated from the sampling area, 52 strains were identified as potential toxin producers, collected from stations 5, 11, 39 and 45. Detailed plate pattern analyses (Supplementary Figures S7-11) combined with molecular

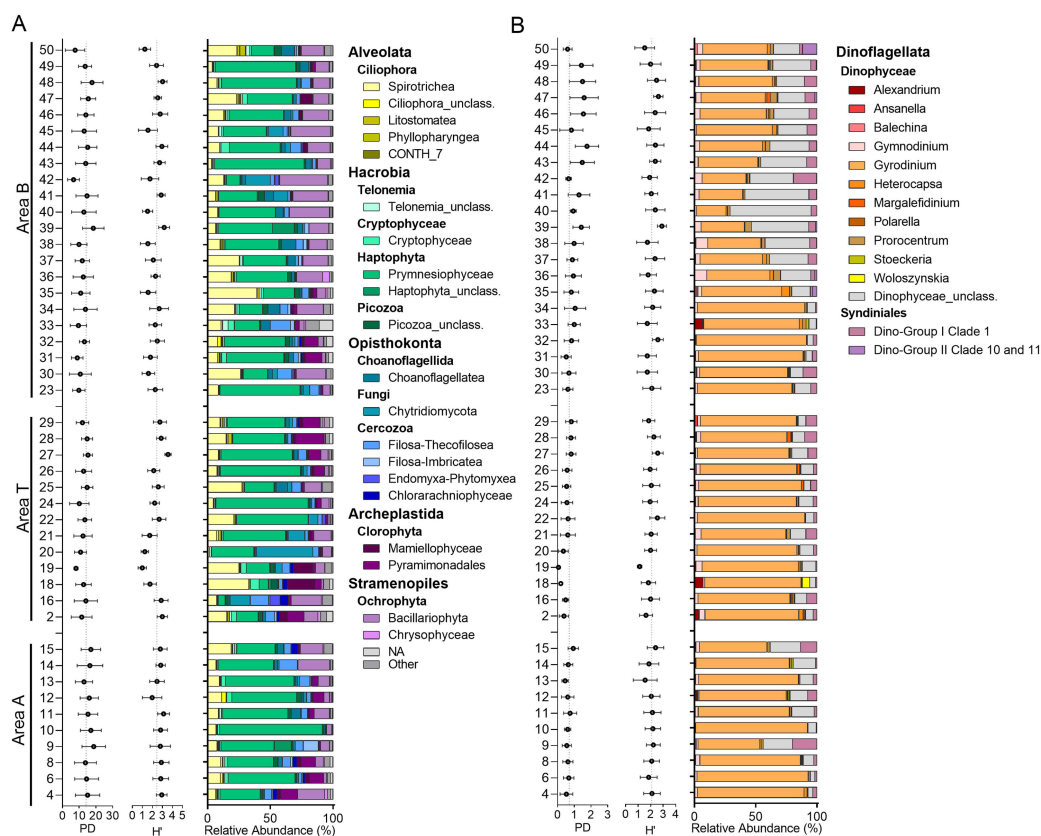


FIGURE 4

Microbial eukaryotic plankton diversity and community composition at each sampling station. Diversity is expressed as average and standard deviation. Faith's Phylogenetic Diversity (PD) and Shannon (H') index for each station. Dashed lines show average values among all areas for each index. Stacked bars show the average (among different depths and size fractions) relative abundance of each station. Only eukaryotic classes with at least 1% of relative abundance are displayed. (A) Other than Dinoflagellata, differentiated by Supergroups, with taxonomic composition at the class level. (B) Dinoflagellata division, differentiated by class, with taxonomic composition at the genus level (when possible). NA: not assigned eukaryotes, Other: classes<1%, Dinophyceae_unclass.: ASVs classified only at the Division level.

identification (Supplementary Table S5) identified these strains as two strains of *Gonyaulax* (with ITS and LSU sequences with 100% identity to *Gonyaulax elongata*), 7 strains of *P. reticulatum*, 11 strains of *A. ostenfeldii*, 11 strains of *A. catenella*, and 21 strains of *A. tamutum* (Supplementary Table S5).

None of the *A. tamutum* strains contained detectable PSTs at detection limits between 0.005 and 0.7 pg cell⁻¹ depending on the toxin variant and available biomass (for details see Supplementary Table S7), while all *A. catenella* strains produced PSP toxins. The toxin profiles of *A. catenella* strains isolated from area A were primarily composed of GTX-2/3 (ca. 50%) and STX (ca. 20%), with minor proportions of GTX-1/4 (except strain MX-C6). In contrast, strains isolated from area B showed completely different PST profiles, dominated by GTX-1/4 (Figure 6A).

All *A. ostenfeldii* strains lacked detectable PSTs and GYMs above their maximum detection levels but produced various SPX compounds, showing marked differentiation between areas. Strains from area A predominantly produced SPX-C and 20-Me-SPX G, comprising about 90% of their SPX profiles. Notably, strain MX-D9/5 contained 90% SPX C but no 20-Me-SPX G. On the other side, *A. ostenfeldii* strains from area B showed a higher diversity of SPX analogs divided into two profiles: strains MX-H11, MX-S-B10, and

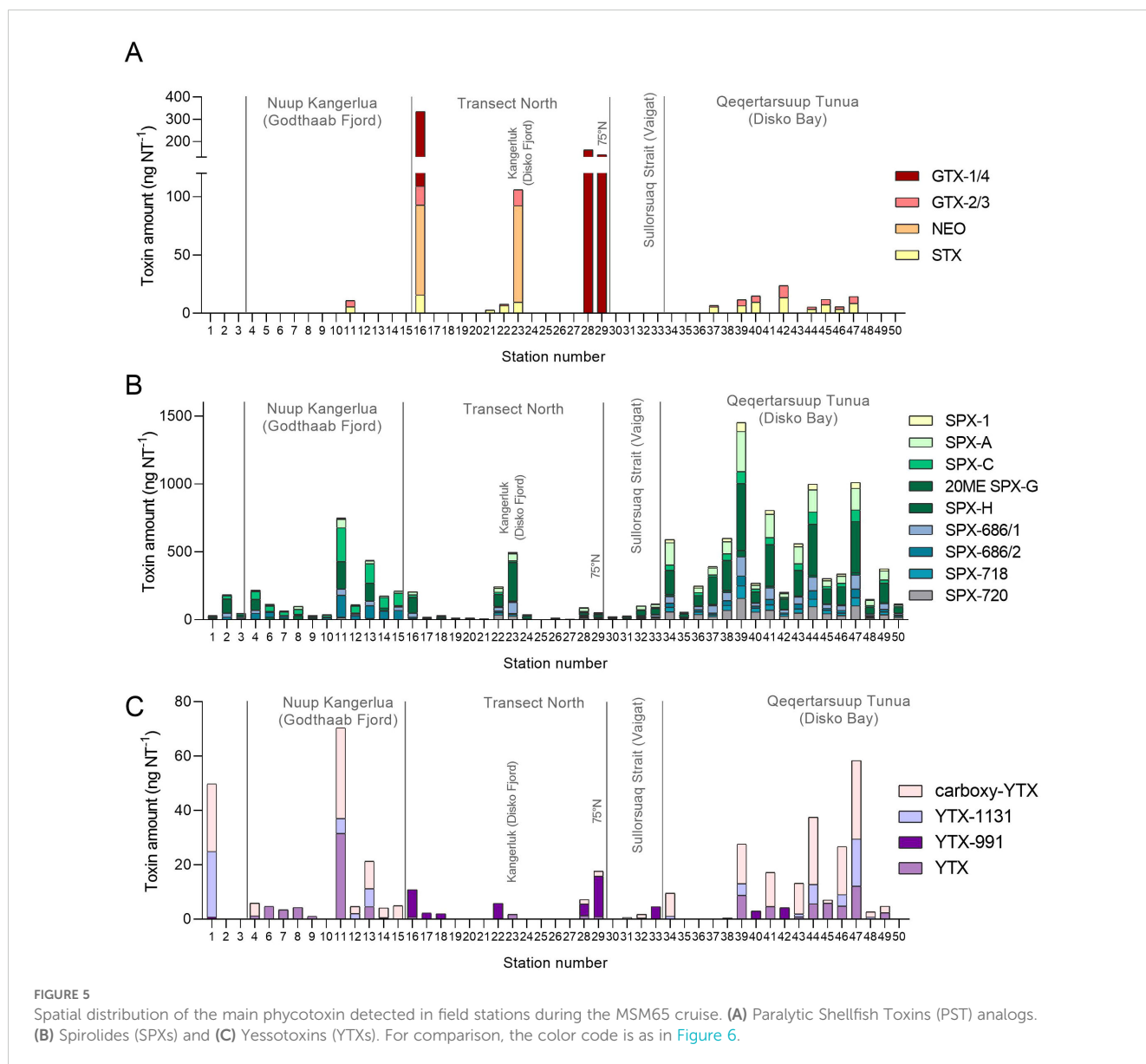
MX-S-B11 were dominated by SPX A and SPX C or 20-Me-SPX G, while strains MX-S-F4, MX-S-F10, and MX-S-F11 were dominated by SPX-1, SPX-718, and SPX-720 (Figure 6B).

All seven strains of *P. reticulatum* contained YTX as the major analogue, comprising over 95% of total YTXs, along with minor amounts of six YTX variants: keto-YTX, nor-YTX, dihydroxy-YTX, and YTX-1159 (corresponding to entry #45 in Miles et al. (2005), YTX-1189 (corresponding to entry #61 or #62), and YTX-1273 (entry #75) (Figure 6C). The YTX profiles of strains from areas A and B were very consistent, showing little variation among isolated strains. For the two strains of *Gonyaulax elongata* no YTXs were detected above the detection limit.

4 Discussion

4.1 Diversity and community composition of microbial eukaryotic plankton in the West Kalaallit Nunaat (Greenland) coast

Overall, our high throughput sequencing results indicate that the Dinoflagellata division outnumber all other planktonic members



throughout the dataset. This dominance is likely due to the high ribosomal copy numbers associated with this lineage (Gong and Marchetti, 2019), as microscopy counts did not indicate a similarly high abundance of dinoflagellates during the cruise. Consequently, we analyzed the diversity and community composition separating the division Dinoflagellata from other plankton members.

Phaeocystis appears as one of the dominant members of the eukaryotic community within the plankton in the West Kalaallit Nunaat (Greenland) coast. Previous studies in this area described differences in plankton community structure and in chemical and physical gradients between the offshore West Greenland and inland regions close to the Greenland Ice Sheet, also showing that *Phaeocystis pouchetii* dominates the phytoplankton community (Arendt et al., 2010). *Phaeocystis* is also a common component of spring blooms around other locations from the Arctic ecosystem, like Svalbard Archipelago and Norway (Verity et al., 2007; Hegseth and Tverberg, 2013).

Particularly in Nuup Kangerlua (Godthaab Fjord), which is located deep inland and begins as an icefjord with two glaciers draining the Greenland ice sheet flowing into the fjord, *Phaeocystis* was found to be associated with cold and relatively saline waters (Krawczyk et al., 2015, 2018). Additionally, centric diatoms, specifically *Chaetoceros* and *Thalassiosira*, were also prevalent in this area, confirming previous findings (Krawczyk et al., 2014).

There is increasing evidence on the importance of heterotrophs and mixotrophs particular in polar areas given their capacity to overcome dark winter periods using phagotrophy as their main carbon acquisition strategy in the absence of light (Stoecker and Lavrentyev, 2018; Søgaard et al., 2021). Heterotrophic and mixotrophic eukaryotes such as Ciliophora, Cercozoa and Dinoflagellates were found to be very abundant in our sequencing data, including the picoplankton size fraction. Considering that there are no described species of Ciliophora, Cercozoa and Dinoflagellates from this size class it would be important to better

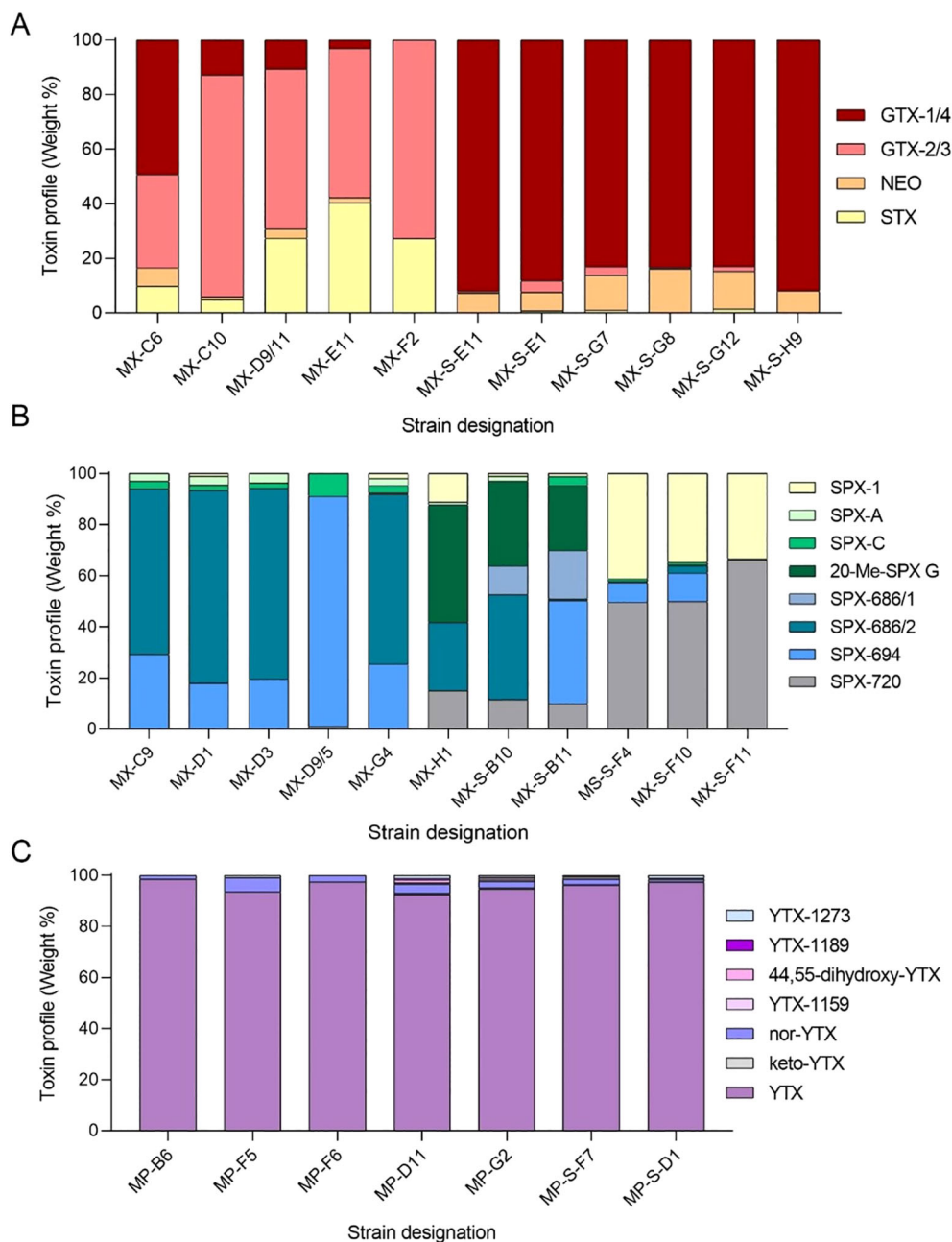


FIGURE 6

Microalgal strains isolated during the MSM65 Cruise and toxin profiles of the producers. (A) Paralytic Shellfish Toxins (PSTs) produced by strains of *Alexandrium catenella*, (B) Spirolides (SPXs) produced by strains of *A. ostenfeldii* and (C) Yesotoxins (YTXs) produced by strains of *Protoceratium reticulatum*. For comparison, color codes are as in Figure 5.

determine how size fractionation biases may distort our view of diversity in different size classes and future assessments are needed to determine whether this phenomenon is due to DNA released from broken cells or if there is a hidden diversity that escaped microscopy analyses and remains to be described.

There are several biases associated with high throughput sequencing of ribosomal markers, including the uneven distribution of 18S rRNA gene copy number among different eukaryote clades (Gong and Marchetti, 2019) and the incompleteness of ribosomal databases, which fortunately are being constantly improved. Despite

these biases, massive sequencing provides a time effective technique to characterize smaller planktonic size fraction that are difficult to identify using morphological traits. In this study, we show that *Micromonas* is the dominant taxa within the picoplanktonic fraction. *Micromonas* has been previously described as a major component at Norwegian and Barents Sea (Not et al., 2005), central Arctic Ocean (Kilian et al., 2014) Beaufort Sea (Lovejoy et al., 2007; Balzano et al., 2012). However, this is the first description of the distribution and relative abundance of this taxon along the West Kalaallit Nunaat (Greenland).

Complementing high throughput sequencing with microscopy allows the identification of taxa that are often difficult to detect with current molecular markers. The quantitative microscopy analysis revealed a list of 92 micro- and nanoplanktonic taxa. For very species-rich groups, such as the dinoflagellate *Protoperidinium* or unarmored dinoflagellate species that in most cases cannot be reliably identified in fixed samples, the actual species diversity without doubt is much higher, as it was also shown by our photo-documentation based on living specimens (Supplementary Figures S3, S4) and sequencing data (Figure 4). Scanning Electron Microscopy examination from field samples suggests that several species of Amphidomatacea, including the newly described *Azadinum perforatum* and other yet undescribed ones, co-occur in the area (Tillmann et al., 2020). Extending strain establishment during future sampling campaigns on rarely studied groups, such as small naked dinoflagellates, will certainly increase knowledge of the protist diversity in the area.

Despite there was vertical distribution in nitrate and phosphate, biomass and Chl-a, our sequencing data show that the composition of eukaryotic taxa was homogeneously distributed throughout the water column and along the West Kalaallit Nunaat (Greenland) coast. This finding, together with the high diversity indices and wide richness of phytoplanktonic classes representing all known divisions, highlights the importance of the microbial dynamics occurring at this threatened ecosystem.

4.2 Phycotoxin distribution in field samples and comparison with toxin profiles from phytoplankton strains

Confirming earlier reports (Baggesen et al., 2012; Tillmann et al., 2016), PSTs were found at various locations without detection of *N*-sulfocarbamoyl (B- and C-) toxins in both isolated strains and field samples. Toxin profiles without *N*-sulfocarbamoyl have been described mainly for the more temperate species *A. minutum* (Chang et al., 1997; Touzet et al., 2008; Liu et al., 2022). The absence of *N*-sulfocarbamoyl toxins in field samples from Western Kalaallit Nunaat (Greenland) suggests the presence of genetically distinct populations of *A. catenella* in this Arctic region in contrast to temperate areas, where *N*-sulfocarbamoyl toxins are typically found in *A. catenella*, often as the major PST variants (Oshima et al., 1992; Krock et al., 2007; Collins et al., 2009). We identified two distinct PST profiles: one profile was dominated almost exclusively by *NI*-OH PSTs (GTX-1/4 and NEO) at coastal stations outside fjords and a second profile solely consisting of *NI*-H PSTs (GTX-2/3 and STX). This trend was also seen in strains isolated in 2012 in Western Kalaallit Nunaat (Greenland) outside Qeqertarsuup Tunua (Disko Bay) and at two coastal stations south of Qeqertarsuup Tunua (Disko Bay), which were also dominated by *NI*-OH PSTs (Tillmann et al., 2016).

Considering that 22 strains were obtained from *A. tamutum*, this species seems to be abundant in the area. Still, toxin analysis confirmed previous data (Long et al., 2021), including one strain from Greenland (Tillmann et al., 2016), that this is a non-PST-producing species.

Like PSTs, the profiles of SPXs showed short-scale regional patterns. The abundance of SPXs is consistent with the fact that the

producing species, *A. ostenfeldii*, is regarded as a boreal species, although it also occurs in temperate regions (Mckenzie et al., 1996; Ciminiello et al., 2007). Notably, in Nuup Kangerlua (Godthaab Fjord), SPX C was more abundant than SPX A, and it was just the opposite in Qeqertarsuup Tunua (Disko Bay). PST profiles of the isolated *A. catenella* strains does not mirror those of the field samples. For example, PSTs were only detected at station 11 in Nuup Kangerlua (Godthaab Fjord) and only the *NI*-H variants were present. In contrast, all strains isolated from the same station primarily produced *NI*-OH variants. One possible explanation for this discrepancy is that local populations of *A. catenella* are composed of different genotypes.

The variability in SPX profiles further show that different genotypes of toxin-producing phytoplankton are present along the West coast of Greenland. Notably, SPX variants found in the field samples and isolated strains were not always identical. For example, SPX H was detected in field samples but not in isolated strains, while SPX-694 was only found in some of the isolated strains but not in any field samples. The strains isolated from Qeqertarsuup Tunua (Disko Bay) at stations 39 and 45 display much more diverse SPX profiles compared to field samples, which reflect the total profiles present at one station and do not necessarily represent the toxin profile of individual or multiple strains isolated from the same station. This discrepancy between field and cultured toxin profiles can be explained by differences in biomass, since minor compounds are easily detectable in the high biomass of isolated strain samples.

Mismatches between field profiles and those of isolated strains was also observed in the case of YTXs. All seven strains isolated in Nuup Kangerlua (Godthaab Fjord) at station 11 and in Qeqertarsuup Tunua (Disko Bay) at station 45 exhibited nearly identical profiles dominated by yessotoxin (YTX), which is typical for *P. reticulatum* (Satake et al., 1997). Interestingly, the YTX profiles of the *P. reticulatum* strains only matched the field profiles of stations 6-9; at all other stations, YTX did not exceed 50% of total YTXs, in most cases even less (Figure 5C). It is also unexpected that none of the three YTXs variants present in the field samples, except YTX itself, were identified among the six YTX variants present in the isolated strains. While some species and strains of the genus *Gonyaulax* have been shown to produce YTXs (Rhodes et al., 2006; Álvarez et al., 2016; Chikwililwa et al., 2019), both strains of *Gonyaulax* (*G. elongata*) lack any detectable YTX, therefore, there is no evidence to support that sub-Arctic populations of *Gonyaulax* contribute to the YTXs found in the field samples.

4.3 Correlation of plankton community composition and oceanographic conditions and how this interaction determines toxin producer species

The low Chl-a concentrations recorded in this study suggest that our sampling during the MSM65 cruise was conducted immediately after the peak of the spring bloom and before the onset of the summer bloom. Previous studies reported that *Chaetoceros* dominate the diatom community at the outer section

of the Nuup Kangerlua (Godthaab Fjord) during the summer bloom (Krawczyk et al., 2015). Our results corroborated this bloom occurred at the full extent of the fjord (Figure 2), particularly at the inner stations influenced by freshwater input. Future investigations should leverage these findings to establish year-round time series in specific areas, thereby enriching our understanding of seasonal dynamics of microbial eukaryotes and toxin-producer species along the area.

When analyzing the toxin producers and toxins, we found positive correlations between the abundances of PST, SPX, YTX, and PTX-2, cell counts by microscopy and reads assigned to each known toxin producer (Supplementary Table S5), although some correlations for sequence reads were not strong. However, it is important to note that both microscopy and toxin analyses were performed on samples collected from the net tow at depths of 30 m depth to the surface, while high throughput sequencing was applied to samples from discrete depths. The strongest correlation was found between YTX concentration, *P. reticulatum* reads, and cell abundance. Since the other known producer of YTX, *Lingulodinium polyedra* was not detected in the samples, this high correlation suggests that the only producer of YTX in this area is *P. reticulatum*.

Microscopy and high throughput sequencing confirmed the presence of *A. catenella* predominantly in Qeqertarsuup Tunua (Disko Bay). PTX-2 was detected at 11 stations within Qeqertarsuup Tunua (Disko Bay) and Nuup Kangerlua (Godthaab Fjord), with the highest abundance recorded at station 11, which also exhibited the highest cell counts and read numbers for *Dinophysis*. Light microscopy analysis indicated that *D. acuminata* was the dominant species in the area, with lower abundances of *D. norvegica* and rare occurrences of *D. acuta*. The later displayed a strong correlation with PTX-2, suggesting *D. acuta* may primarily produce this phycotoxin in this area.

On the other hand, we observed a notable discrepancy between cell count and sequencing reads of *Pseudo-nitzschia*, and DA amounts (see Supplementary Table S5). The production of DA by *Pseudo-nitzschia* is species-specific (Bates et al., 2018) and influenced by external factors such as nutrient limitation (phosphate or silicate) (Lelong et al., 2012) and by the presence of predators (Lundholm et al., 2018). DA is also known to accumulate in copepods (Leandro et al., 2010). Therefore, the total cell densities of potentially multiple *Pseudo-nitzschia* species do not necessarily correspond to particulate toxin levels. Besides, *Pseudo-nitzschia* have been shown to distribute in thin layers, evading traditional sampling schemes, which has been proposed as a camouflage mechanism hiding *Pseudo-nitzschia* populations (Rines et al., 2002). This highlights the importance of recognizing that discrete sampling may not accurately reflect the true distribution of certain plankton species within the water column.

Glacier melting has several effects on the water column. Key parameters for the marine ecosystem include decreasing salinity and consequent stratification, nutrient input and light availability, all of which are more complex in fjord systems.

In Qeqertarsuup Tunua (Disko Bay) the distribution of PAR 1% was initially unintuitive, as light penetration was deeper just before the Sermeq Kujalleq (Jacobshavn Isbraer) outlet glacier, that contributes 85% of freshwater discharge into the Ilulissat Kangerlua (Mernild et al.,

2015). However, the glacial waters that turn northward through the Vaigat and the central Disko Bay have a circulating pattern that seems to preserve water insight with low productivity (Supplementary Figure S1) and more transparent water than towards the shores. This dynamic seems to have an enhancing effect in phycotoxin producers, specially *A. ostenfeldii*, since the higher SPX concentrations were recorded at this area, and not at Vaigat Strait, that seem to receive most of the direct glacial input.

At Nuup Kangerlua (Godthaab Fjord) PAR1% depth showed the inhibiting effects on light penetration due to glacial sediments suspended in the water column (Supplementary Figure S2). This effect was also reflected in the silicic acid concentration, salinity, and temperature at stations 9 and 10, which were close to the glacier outlet. These stations exhibited higher nutrient and Chl-a concentrations than the rest of the Fjord. Toxins detected (SPX and YTX) were not high at these stations, and the conditions seem to be favorable for diatom growth. Higher concentrations of toxins were found in station 11, that also displayed higher temperature and lower nutrients than other stations at Nuup Kangerlua (Godthaab Fjord). This particular station is enclosed and highly protected, generating suitable growth conditions for toxin-producer dinoflagellates.

Overall, the highest concentration of toxins detected in the current study at Qeqertarsuup Tunua (Disko Bay), were present at stations that were not directly influenced by the turbidity of melted waters. This, combined with the toxin distribution pattern found at Nuup Kangerlua (Gothaab Fjord), suggests that dinoflagellate toxins are more likely to be present in stable and enclosed areas, influenced by glacier melting but not directly at the glacier outlet, where higher turbidity and silicic acid availability seem to promote diatom but not dinoflagellate growth.

However, when analyzing the link between SPXs, PTX-2, PSTs, and YTXs and oceanographical parameters, we found that each of these phycotoxins correlated different with distinct environmental factors. For instance, SPX were positively correlated with temperature and negatively correlated with salinity and silicic acid, suggesting that they are more likely to be found in highly stratified water bodies or areas with elevated temperatures that are not directly influenced by glacier melted waters. Conversely, the positive correlation of PTX-2 with silicic acid and turbidity suggest that it may be linked to direct glacier melting, as melted glacier water tend to carry high sediment content and silicic acid concentrations, as evidenced at stations 9 and 10, in close proximity to glacier melting. Considering that two phycotoxins groups (SPXs and YTXs) positively correlated with temperature, and as the Arctic Ocean becomes warmer and sea ice diminish, toxin distributions may undergo shift in their extent and distribution. Therefore, permanent monitoring of these variables is highly relevant for the Kalaallit Nunaat (Greenland) ecosystem, where shellfish harvesting are a significant economic source.

5 Conclusions

We found a complex oceanographical system characterized by vertical stratification of physicochemical variables and biomass and a highly diverse and homogeneous microbial eukaryotic communities

dominated by diatoms, haptophytes, and dinoflagellates along coastal waters of Kalaallit Nunaat (Greenland). We identified the sampling period as an inter-bloom summer period, with no significant variation in phytoplankton composition according to depth, size, or area according to molecular data. At least, five phycotoxin groups and their producers were identified, with spirolides, yessotoxins and pectenotoxins detected mainly in enclosed areas, freshwater influenced, and domoic acid detected mainly at the northern West Kalaallit Nunaat (Greenland) coast. Our results suggest a high diversity in toxin profile among producers of PST, SPX and YTX, and that detected phycotoxins correlate differently with temperature, salinity and nutrients. The risk associated to phycotoxins is likely to increase due to the effects of global warming, rising seawater temperatures, and increased glacier melting, as most toxin producers thrive at freshwater-influenced zones. Given that the human population of Kalaallit Nunaat (Greenland) relies significantly on marine resources, there is an urgent need for integrating research and monitoring of HAB species and their impacts on human health and marine fauna.

Data availability statement

The datasets generated in this study can be found in the SRA repository. Nucleotide sequence accession numbers are PRJNA1046074 (Available at: <https://www.ncbi.nlm.nih.gov/bioproject/?term=PRJNA1046074>) for 18S rRNA gene and PRJNA1052066 (<https://www.ncbi.nlm.nih.gov/bioproject/?term=PRJNA1052066>) for isolated strains.

Author contributions

SR: Formal analysis, Methodology, Software, Visualization, Writing – original draft, Writing – review & editing. BK: Conceptualization, Formal analysis, Funding acquisition, Investigation, Methodology, Supervision, Writing – original draft, Writing – review & editing. UT: Conceptualization, Formal analysis, Investigation, Methodology, Writing – review & editing. AT: Formal analysis, Investigation, Writing – review & editing. DV: Formal analysis, Investigation, Methodology, Visualization, Writing – review & editing. OZ: Conceptualization, Funding acquisition, Investigation, Supervision, Writing – review & editing. MV: Writing – review & editing, Methodology. NT: Conceptualization, Formal analysis, Funding acquisition, Investigation, Supervision, Writing – original draft, Writing – review & editing, Methodology.

Funding

The author(s) declare financial support was received for the research, authorship, and/or publication of this article. This work was supported by the UMayor initiatives ‘Puente’ and ‘Proyectos especiales’ from the Vicerrectoria de Investigación (2017) and Fondecyt N°1230758 (to NT), DynAMo (01 DN17045), from the German Federal Ministry of Education and Science (BMBF) and the

European Union’s Horizon 2020 research and innovation program under the Marie Skłodowska-Curie grant agreement No 872690. Furthermore, this work was funded by the Helmholtz-Gemeinschaft Deutscher Forschungszentren through the research program PACES II of the Alfred-Wegener-Institut–Helmholtz Zentrum für Polar- und Meeresforschung.

Acknowledgments

We acknowledge the crew of the R/V Maria S. Merian and scientific personnel during the MSM65 cruise. We thank Nathalie Delherbe, Marlene Manzano, and Génesis Parada-Pozo for logistic support for the campaign preparation, flow cytometry measurements, and DNA extractions. We thank Anne Müller, Thomas Max and Rohan Henkel for their technical support onboard sampling and toxin analyses. The support of Kerstin Klemm for PCR confirmation of strain identity is very much acknowledged. Stephan Wietkamp and Anne Müller assisted with microalgal strain DNA extraction and marker gene sequencing.

Conflict of interest

The authors declare that the research was conducted in the absence of any commercial or financial relationships that could be construed as a potential conflict of interest.

Publisher’s note

All claims expressed in this article are solely those of the authors and do not necessarily represent those of their affiliated organizations, or those of the publisher, the editors and the reviewers. Any product that may be evaluated in this article, or claim that may be made by its manufacturer, is not guaranteed or endorsed by the publisher.

Supplementary material

The Supplementary Material for this article can be found online at: <https://www.frontiersin.org/articles/10.3389/fmars.2024.1443389/full#supplementary-material>

SUPPLEMENTARY FIGURE 1
PAR 1% depth.

SUPPLEMENTARY FIGURE 2
Mean environmental parameters from surface to the Deep Chlorophyll Maximum (S, aDCM and DCM). Light microscopy micrographs of living specimen on the left side are included to exemplify the species and the diversity in the respective plankton category. (A) *Phaeocystis pouchetii* abundance ($n L^{-1}$). (B) *Dinobryon balticum* abundance ($n L^{-1}$). (C) Biomass of other flagellates (without *P. pouchetii* and *D. balticum*, also excluding all

SUPPLEMENTARY FIGURE 3

Distribution of selected species/groups of plankton based on microscopic quantification of pooled water samples from 3m, 10m, and Deep Chlorophyll Maximum (S, aDCM and DCM). Light microscopy micrographs of living specimen on the left side are included to exemplify the species and the diversity in the respective plankton category. (A) *Phaeocystis pouchetii* abundance ($n L^{-1}$). (B) *Dinobryon balticum* abundance ($n L^{-1}$). (C) Biomass of other flagellates (without *P. pouchetii* and *D. balticum*, also excluding all

dinoflagellates ($\mu\text{g C L}^{-3}$). (D) Biomass of dinoflagellate species known to have plastids ($\mu\text{g C L}^{-3}$). (E) Biomass of dinoflagellate species known to lack plastids ($\mu\text{g C L}^{-3}$). (F) Biomass of ciliates ($\mu\text{g C L}^{-3}$). Note that the bar chart separates the mixotrophic species *Mesodinium rubrum* from other ciliates. (G) *Pseudo-nitzschia* spp. abundance (n L^{-3}). (H) Pennate diatoms (other than *Pseudo-nitzschia* spp.) abundance (n L^{-3}). (I) *Thalassiosira* spp. abundance (n L^{-3}). (J) abundance of small *Chaetoceros* spp. (n L^{-3}). Note that the majority of counts likely refers to the colonial species *C. socialis*. (K) Biomass of other *Chaetoceros* spp. ($\mu\text{g C L}^{-3}$). Note that the biomass peaks are mainly due to high densities of *Chaetoceros debilis*.

SUPPLEMENTARY FIGURE 4

Potentially toxic plankton genera including species of *Prymnesium* (A–C), *Pseudo-nitzschia* (D), *Pseudo-nitzschia* (E, F), *Dinophysis* (G–K), *Azadinium* (L), *Karlodinium* (M, N), *Margalefidinium* (O–Q), *Alexandrium* (R–V), *Protoceratium* (W), and *Gonyaulax* (X–Z).

SUPPLEMENTARY FIGURE 5

Beta diversity analyses for other microbial eukaryotes and dinoflagellate community composition at ASV level.

SUPPLEMENTARY FIGURE 6

Marine toxins detected in each study area.

SUPPLEMENTARY FIGURE 7

Gonyaulax elongata morphology of cultured strain.

SUPPLEMENTARY FIGURE 8

Protoceratium reticulatum morphology of cultured strains.

SUPPLEMENTARY FIGURE 9

Alexandrium ostenfeldii (strain MX-SB11) in brightfield (A–E) or squeezed thecal plates stained with solophenylflavine viewed in fluorescence light (F–L).

SUPPLEMENTARY FIGURE 10

Alexandrium catenella (strain MX-C11) in brightfield (A–D) or thecal plates stained with solophenylflavine viewed in fluorescence light (E–U).

SUPPLEMENTARY FIGURE 11

Alexandrium tamutum (strain MX-F3) in brightfield (A–D) or thecal plates stained with solophenylflavine viewed in fluorescence light (E–Q).

References

- Álvarez, G., Uribe, E., Regueiro, J., Blanco, J., and Fraga, S. (2016). *Gonyaulax taylorii*, a new yessotoxins-producer dinoflagellate species from Chilean waters. *Harmful Algae* 58, 8–15. doi: 10.1016/j.hal.2016.07.006
- Arar, E. J., and Collins, G. B. (1997). *Method 445.0 In Vitro Determination of Chlorophyll a and Pheophytin a in Marine and Freshwater Algae by Fluorescence* (Cincinnati, Ohio: U.S. Environmental Protection Agency). ed. W. D.
- Arendt, K. E., Nielsen, T. G., Rysgaard, S., and Tønnesson, K. (2010). Differences in plankton community structure along the Godthåbsfjord, from the Greenland Ice Sheet to offshore waters. *Mar. Ecol. Progress Series* 401, 49–62. doi: 10.3354/meps08368
- Arrigo, K. R., van Dijken, G. L., Castelao, R. M., Luo, H., Rennermalm, Å.K., Tedesco, M., et al. (2017). Melting glaciers stimulate large summer phytoplankton blooms in southwest Greenland waters. *Geophys. Res. Lett.* 44, 6278–6285. doi: 10.1002/2017GL073583
- Baggesen, C., Moestrup, Ø., Daugbjerg, N., Krock, B., Cembella, A. D., and Madsen, S. (2012). Molecular phylogeny and toxin profiles of *Alexandrium tamarense* (Lebour) Balech (Dinophyceae) from the west coast of Greenland. *Harmful Algae* 19, 108–116. doi: 10.1016/j.hal.2012.06.005
- Balzano, S., Gourvil, P., Siano, R., Chanoine, M., Marie, D., Lessard, S., et al. (2012). Diversity of cultured photosynthetic flagellates in the northeast Pacific and Arctic Oceans in summer. *Biogeosciences* 9, 4553–4571. doi: 10.5194/bg-9-4553-2012
- Bates, S. S., Hubbard, K. A., Lundholm, N., Montresor, M., and Leaw, C. P. (2018). *Pseudo-nitzschia*, *Nitzschia*, and domoic acid: New research since 2011. *Harmful Algae* 79, 3–43. doi: 10.1016/j.hal.2018.06.001
- Berdal, E., Fleming, L. E., Gowen, R., Davidson, K., Hess, P., Backer, L. C., et al. (2015). Marine harmful algal blooms, human health and wellbeing: challenges and opportunities in the 21st century. *J. Mar. Biol. Assoc. United Kingdom* 96 (1), 61–91. doi: 10.1017/S0025315415001733
- Bruhn, C. S., Wohlrab, S., Krock, B., Lundholm, N., and John, U. (2021). Seasonal plankton succession is in accordance with phycotoxin occurrence in Disko Bay, West Greenland. *Harmful Algae* 103, 101978. doi: 10.1016/j.hal.2021.101978
- Callahan, B. J., McMurdie, P. J., and Holmes, S. P. (2017). Exact sequence variants should replace operational taxonomic units in marker-gene data analysis. *ISME J.* 11, 2639–2643. doi: 10.1038/ismej.2017.119
- Chang, F. H., Anderson, D. M., Kulis, D. M., and Till, D. G. (1997). Toxin production of *Alexandrium minutum* (Dinophyceae) from the Bay of Plenty, New Zealand. *Toxicon* 35, 393–409. doi: 10.1016/S0041-0101(96)00168-7
- Chikwililwa, C., McCarron, P., Waniek, J. J., and Schulz-Bull, D. E. (2019). Phylogenetic analysis and yessotoxin profiles of *Gonyaulax spinifera* cultures from the Benguela Current upwelling system. *Harmful Algae* 85, 101626. doi: 10.1016/j.hal.2019.101626
- Ciminiello, P., Dell'Aversano, C., Fattorusso, E., Forino, M., Grauso, L., Tartaglione, L., et al. (2007). Spiroliide toxin profile of adriatic *Alexandrium ostenfeldii* cultures and structure elucidation of 27-hydroxy-13,19-didesmethyl spiroliide C. *J. Nat. Prod.* 70, 1878–1883. doi: 10.1021/np0703242
- Collins, C., Graham, J., Brown, L., Bresnan, E., Lacaze, J. P., and Turrell, E. A. (2009). Identification and toxicity of *Alexandrium tamarense* (dinophyceae) in Scottish waters. *J. Phycol.* 45, 692–703. doi: 10.1111/j.1529-8817.2009.00678.x
- Comeau, A. M., Li, W. K. W., Tremblay, J.É., Carmack, E. C., and Lovejoy, C. (2011). Arctic ocean microbial community structure before and after the 2007 record sea ice minimum. *PLoS One* 6 (11), e27492. doi: 10.1371/journal.pone.0027492
- Diener, M., Erler, K., Christian, B., and Luckas, B. (2007). Application of a new zwitterionic hydrophilic interaction chromatography column for determination of paralytic shellfish poisoning toxins. *J. Sep. Sci.* 30, 1821–1826. doi: 10.1002/jssc.200700025
- Elferink, S., Neuhaus, S., Wohlrab, S., Toebe, K., Voß, D., Gottschling, M., et al. (2017). Molecular diversity patterns among various phytoplankton size-fractions in West Greenland in late summer. *Deep Sea Res. 1 Oceanogr. Res. Pap.* 121, 54–69. doi: 10.1016/j.dsr.2016.11.002
- Elferink, S., Wohlrab, S., Neuhaus, S., Cembella, A., Harms, L., and John, U. (2020). Comparative metabarcoding and metatranscriptomic analysis of microeukaryotes within coastal surface waters of West Greenland and Northwest Iceland. *Front. Mar. Sci.* 7. doi: 10.3389/fmars.2020.00439
- Gobler, C. J. (2020). Climate change and harmful algal blooms: insights and perspective. *Harmful Algae* 91, 101731. doi: 10.1016/j.hal.2019.101731
- Gong, W., and Marchetti, A. (2019). Estimation of 18S gene copy number in marine eukaryotic plankton using a next-generation sequencing approach. *Front. Mar. Sci.* 6. doi: 10.3389/fmars.2019.00219
- Graeve, M., Ludwiczowski, K.-U., and Leefmann, T. (2018). *Inorganic nutrients measured on water bottle samples from CTD/Water sampler-system during MARIA S.MERIAN cruise MSM65 (GREENHAB II). Alfred Wegener Institute, Helmholtz Centre for Polar and Marine Research, Bremerhaven (Bremerhaven, Germany: PANGAEA).* doi: 10.1594/PANGAEA.887413
- Guillou, L., Bachar, D., Audic, S., Bass, D., Berney, C., Bittner, L., et al. (2013). The Protist Ribosomal Reference database (PR2): A catalog of unicellular eukaryote Small Sub-Unit rRNA sequences with curated taxonomy. *Nucleic Acids Res.* 41 (D1), D597–D604. doi: 10.1093/nar/gks1160
- Hallegraef, G., Enevoldsen, H., and Zingone, A. (2021). Global harmful algal bloom status reporting. *Harmful Algae* 102, 101992. doi: 10.1016/j.hal.2021.101992
- Hammer, D. A. T., Ryan, P. D., Hammer, Ø., and Harper, D. A. T. (2001). Past: paleontological statistics software package for education and data analysis. *Palaeontol Electron* 4, 9. doi: 10.1016/j.bcp.2008.05.025
- Hansen, L. R., Soylu, S.İ., Kotaki, Y., Moestrup, Ø., and Lundholm, N. (2011). Toxin production and temperature-induced morphological variation of the diatom *Pseudo-nitzschia seriata* from the Arctic. *Harmful Algae* 10, 689–696. doi: 10.1016/j.hal.2011.05.004
- Hegseth, E. N., and Tverberg, V. (2013). Effect of Atlantic water inflow on timing of the phytoplankton spring bloom in a high Arctic fjord (Kongsfjorden, Svalbard). *J. Mar. Syst.* 113, 94–105. doi: 10.1016/j.jmarsys.2013.01.003
- Heide-Jørgensen, M. P., Laidre, K. L., Logsdon, M. L., and Nielsen, T. G. (2007). Springtime coupling between chlorophyll a, sea ice and sea surface temperature in Disko Bay, West Greenland. *Prog. Oceanogr.* 73, 79–95. doi: 10.1016/j.pocean.2007.01.006
- Juul-Pedersen, T., Arendt, K. E., Mortensen, J., Blicher, M. E., Søgaard, D. H., and Rysgaard, S. (2015). Seasonal and interannual phytoplankton production in a sub-Arctic tidewater outlet glacier fjord, SW Greenland. *Mar. Ecol. Prog. Ser.* 524, 27–38. doi: 10.3354/meps11174
- Keller, M. D., Seluín, R. C., Claus, W., and Guillard, R. R. L. (1987). Media for the culture of oceanic Ultraphytoplankton. *J. Phycol.* 23 (4), 633–638. doi: 10.1111/j.1529-8817.1987.tb04217.x
- Kembel, S. W., Cowan, P. D., Helmus, M. R., Cornwell, W. K., Morlon, H., Ackerly, D. D., et al. (2010). Picante: R tools for integrating phylogenies and ecology. *Bioinformatics* 26, 1463–1464. doi: 10.1093/bioinformatics/btq166

- Kilias, E., Kattner, G., Wolf, C., Frickenhaus, S., and Metfies, K. (2014). A molecular survey of protist diversity through the central Arctic Ocean. *Polar Biol.* 37, 1271–1287. doi: 10.1007/s00300-014-1519-5
- Krawczyk, D. W., Meire, L., Lopes, C., Juul-Pedersen, T., Mortensen, J., Li, C. L., et al. (2018). Seasonal succession, distribution, and diversity of planktonic protists in relation to hydrography of the Godthåbsfjord system (SW Greenland). *Polar Biol.* 41, 2033–2052. doi: 10.1007/s00300-018-2343-0
- Krawczyk, D. W., Witkowski, A., Juul-Pedersen, T., Arendt, K. E., Mortensen, J., and Rysgaard, S. (2015). Microplankton succession in a SW Greenland tidewater glacial fjord influenced by coastal inflows and run-off from the Greenland Ice Sheet. *Polar Biol.* 38, 1515–1533. doi: 10.1007/s00300-015-1715-y
- Krawczyk, D. W., Witkowski, A., Waniek, J. J., Wroniecki, M., and Harff, J. (2014). Description of diatoms from the Southwest to West Greenland coastal and open marine waters. *Polar Biol.* 37, 1589–1606. doi: 10.1007/s00300-014-1546-2
- Krock, B., Seguel, C. G., and Cembella, A. D. (2007). Toxin profile of *Alexandrium catenella* from the Chilean coast as determined by liquid chromatography with fluorescence detection and liquid chromatography coupled with tandem mass spectrometry. *Harmful Algae* 6, 734–744. doi: 10.1016/j.hal.2007.02.005
- Krock, B., Tillmann, U., Alpermann, T. J., Vofš, D., Zielinski, O., and Cembella, A. D. (2013). Phycotoxin composition and distribution in plankton fractions from the German Bight and western Danish coast. *J. Plankton Res.* 35, 1093–1108. doi: 10.1093/plankt/ftb054
- Krock, B., Tillmann, U., Tebben, J., Trefault, N., and Gu, H. (2019). Two novel azaspiracids from *Azadinium poporum*, and a comprehensive compilation of azaspiracids produced by Amphidomataceae, (Dinophyceae). *Harmful Algae* 82, 1–8. doi: 10.1016/j.hal.2018.12.005
- Leandro, L. F., Teegarden, G. J., Roth, P. B., Wang, Z., and Doucette, G. J. (2010). The copepod *Calanus finmarchicus*: A potential vector for trophic transfer of the marine algal biotoxin, domoic acid. *J. Exp. Mar. Biol. Ecol.* 382, 88–95. doi: 10.1016/j.jembe.2009.11.002
- Lee, S., and Fuhrman, J. A. (1987). Relationships between biovolume and biomass of naturally derived marine bacterioplankton. *Appl. Environ. Microbiol.* 53, 1298–1303. doi: 10.1128/aem.53.6.1298-1303.1987
- Lelong, A. L., Hégaret, H.É., Soudant, P., and Bates, S. S. (2012). Pseudo-nitzschia (Bacillariophyceae) species, domoic acid and amnesic shellfish poisoning: revisiting previous paradigms. *Phycologia* 51, 168–216. doi: 10.2216/11-37
- Liu, M., Krock, B., Yu, R., Leaw, C. P., Lim, P. T., Ding, G., et al. (2022). Co-occurrence of *Alexandrium minutum* (Dinophyceae) ribotypes from the Chinese and Malaysian coastal waters and their toxin production. *Harmful Algae* 115, 102238. doi: 10.1016/j.hal.2022.102238
- Long, M., Krock, B., Castrec, J., and Tillmann, U. (2021). Unknown extracellular and bioactive metabolites of the genus *Alexandrium*: A review of overlooked toxins. *Toxins (Basel)* 13 (12), 905. doi: 10.3390/toxins13120905
- Lovejoy, C., Vicent, W. F., Bonilla, S., Roy, S., Martineau, M. J., Potvin, M., et al. (2007). Distribution, phylogeny, and growth of cold-adapted Picoprasinophytes in Arctic Seas. *J. Phycol.* 43, 78–89. doi: 10.1111/j.1529-8817.2006.00310.x
- Lundholm, N., Krock, B., John, U., Skov, J., Cheng, J., Pančić, M., et al. (2018). Induction of domoic acid production in diatoms—Types of grazers and diatoms are important. *Harmful Algae* 79, 64–73. doi: 10.1016/j.hal.2018.06.005
- Marie, D., Simon, N., and Vaulot, D. (2005). Phytoplankton cell counting by flow cytometry. *Algal culturing techniques* 1, 253–267. doi: 10.1016/b978-012088426-1/50018-4
- Marquardt, M., Vader, A., Stübner, E. I., Reigstad, M., and Gabrielsen, T. M. (2016). Strong seasonality of marine microbial eukaryotes in a high-Arctic fjord (Isfjorden, in West Spitsbergen, Norway). *Appl. Environ. Microbiol.* 82, 1868–1820. doi: 10.1128/AEM.03208-15
- Martin, M. (2011). Cutadapt removes adapter sequences from high-throughput sequencing reads. *EMBnet journal* 17 (1), 10–12. doi: 10.14806/ebj.17.1.200
- Mckenzie, L., Whitei, D., Oshima, Y., Kapa, J., Mackenzie, L., White, D., et al. (1996). The resting cyst and toxicity of *Alexandrium ostenfeldii* (Dinophyceae) in New Zealand. *Phycologia* 35 (2), 148–155. doi: 10.2216/i0031-8884-35-2-148.1
- Meire, L., Paulsen, M. L., Meire, P., Rysgaard, S., Hopwood, M. J., Sejr, M. K., et al. (2023). Glacier retreat alters downstream fjord ecosystem structure and function in Greenland. *Nat. Geosci* 16, 671–674. doi: 10.1038/s41561-023-01218-y
- Menden-Deuer, S., and Lessard, E. J. (2000). Carbon to volume relationships for dinoflagellates, diatoms, and other protist plankton. *Limnol Oceanogr* 45, 569–579. doi: 10.4319/lo.2000.45.3.0569
- Mernild, S. H., Holland, D. M., Holland, D., Rosing-Asvid, A., Yde, J. C., Liston, G. E., et al. (2015). Freshwater flux and spatiotemporal simulated runoff variability into Ilulissat Icefjord, West Greenland, linked to salinity and temperature observations near tidewater glacier margins obtained using instrumented ringed seals. *J. Phys. Oceanography* 45, 1426–1445. doi: 10.1175/JPO-D-14-0217.1
- Metfies, K., Von Appen, W. J., Kilias, E., Nicolaus, A., and Nöthig, E. M. (2016). Biogeography and photosynthetic biomass of arctic marine pico-eukaryotes during summer of the record sea ice minimum 2012. *PLoS One* 11(2), e0148512. doi: 10.1371/journal.pone.0148512
- Miles, C. O., Samdal, I. A., Aasen, J. A. G., Jensen, D. J., Quilliam, M. A., Petersen, D., et al. (2005). Evidence for numerous analogs of yessotoxin in *Protoceratium reticulatum*. *Harmful Algae* 4, 1075–1091. doi: 10.1016/j.hal.2005.03.005
- Mortensen, J., Lennert, K., Bendtsen, J., and Rysgaard, S. (2011). Heat sources for glacial melt in a sub-Arctic fjord (Godthåbsfjord) in contact with the Greenland Ice Sheet. *J. Geophys. Res. Oceans* 116 (C1). doi: 10.1029/2010JC006528
- Mueller, J. L., Fargion, G. S., McClain, C. R., Mueller, J. L., Morel, A., Frouin, R., et al. (2003). *Ocean optics protocols for satellite ocean color sensor validation, revision 4, volume III: radiometric measurements and data analysis protocols*. (Greenbelt, MD: Goddard Space Flight Space Centre) pp. 1–84. doi: 10.25607/OBP-62
- Nieva, J. A., Krock, B., Tillmann, U., Tebben, J., Zurhelle, C., and Bickmeyer, U. (2020). Gymnodimine A and 13-desMethyl spirolide C alter intracellular calcium levels via acetylcholine receptors. *Toxins (Basel)* 12 (12), 751. doi: 10.3390/toxins12120751
- Not, F., Massana, R., Latasa, M., Marie, D., Colson, C., Eikrem, W., et al. (2005). Late summer community composition and abundance of photosynthetic picoeukaryotes in Norwegian and Barents Seas. *Limnology Oceanography* 50, 1677–1686. doi: 10.4319/lo.2005.50.5.1677
- Oksanen, J., Kindt, R., Legendre, P., O'Hara, B., Simpson, G. L., Solymos, P., et al. (2022). *Vegan: Community Ecology Package. R package version 2.6.4*. Available online at: <http://cran.r-project.org/>. (Accessed January 10, 2023)
- Organeli, E., Claustre, H., Bricaud, A., Schmechtig, C., Poteau, A., Xing, X., et al. (2016). A novel near-real-time quality-control procedure for radiometric profiles measured by bio-argo floats: Protocols and performances. *J. Atmos Ocean Technol.* 33, 937–951. doi: 10.1175/JTECH-D-15-0193.1
- Oshima, Y. U., Bolch, C. J., and Hallegraef, G. (1992). Toxin composition of resting cysts of *Alexandrium tamarense* (Dinophyceae). *Toxicon* 30 (12), 1539–1544. doi: 10.1016/0041-0101(92)90025-Z
- R Core Team, R. (2018). *R: A Language and Environment for Statistical Computing* (Vienna, Austria: R Foundation for Statistical Computing). Available at: <https://www.R-project.org/>.
- Rhodes, L., McNabb, P., De Salas, M., Briggs, L., Beuzenberg, V., and Gladstone, M. (2006). Yessotoxin production by *Gonyaulax spinifera*. *Harmful Algae* 5, 148–155. doi: 10.1016/j.hal.2005.06.008
- Richlen, M. L., Zielinski, O., Holinde, L., Tillmann, U., Cembella, A., Lyu, Y., et al. (2016). Distribution of *Alexandrium fundyense* (Dinophyceae) cysts in Greenland and Iceland, with an emphasis on viability and growth in the Arctic. *Mar. Ecol. Prog. Ser.* 547, 33–46. doi: 10.3354/meps11660
- Rines, J. E. B., Donaghay, P. L., Deksheniaks, M. M., Sullivan, J. M., and Twardowski, M. S. (2002). Thin layers and camouflage: Hidden *Pseudo-nitzschia* spp. (Bacillariophyceae) populations in a fjord in the San Juan Islands, Washington, USA. *Mar. Ecol. Prog. Ser.* 225, 123–137. doi: 10.3354/meps225123
- Rysgaard, S., Vang, T., Stjernholm, M., Rasmussen, B., Windelin, A., and Kiilsholm, S. (2003). Physical conditions, carbon transport, and climate change impacts in a northeast Greenland fjord. *Arct Antarct Alp Res.* 35, 301–312. doi: 10.1657/1523-0430(2003)035[0301:PCCTAC]2.0.CO;2
- Sala-Pérez, M., Alpermann, T. J., Krock, B., and Tillmann, U. (2016). Growth and bioactive secondary metabolites of arctic *Protoceratium reticulatum* (Dinophyceae). *Harmful Algae* 55, 85–96. doi: 10.1016/j.hal.2016.02.004
- Satake, M., MacKenzie, L., and Yasumoto, T. (1997). Identification of *Protoceratium reticulatum* as the biogenetic origin of yessotoxin. *Natural Toxins* 5, 164–167. doi: 10.1002/19970504NT7
- Sayers, E. W., Bolton, E. E., Brister, J. R., Canese, K., Chan, J., Comeau, D. C., et al. (2022). Database resources of the national center for biotechnology information. *Nucleic Acids Res.* 50, D20–D26. doi: 10.1093/nar/gkab1112
- Schlitzer, R. (2022). *Ocean data view*. Available online at: <https://odv.awi.de> (Accessed November 27, 2023).
- Shapiro, S. S., and Wilk, M. B. (1965). An analysis of variance test for normality (Complete samples). *Biometrika* 52, 591–611. Available at: <https://www.jstor.org/stable/2333709>.
- Sogaard, D. H., Sorrell, B. K., Sejr, M. K., Andersen, P., Rysgaard, S., Hansen, P. J., et al. (2021). An under-ice bloom of mixotrophic haptophytes in low nutrient and freshwater-influenced Arctic waters. *Sci. Rep.* 11, 2915. doi: 10.1038/s41598-021-82413-y
- Stoecker, D. K., and Lavrentyev, P. J. (2018). Mixotrophic plankton in the polar seas: A pan-Arctic review. *Front. Mar. Sci.* 5. doi: 10.3389/fmars.2018.00292
- Straneo, F., and Cenedese, C. (2015). The dynamics of Greenland's glacial fjords and their role in climate. *Ann. Rev. Mar. Sci.* 7, 89–112. doi: 10.1146/annurev-marine-010213-135133
- Sukhanova, I. N., Flint, M. V., Pautova, L. A., Stockwell, D. A., Grebmeier, J. M., and Sergeeva, V. M. (2009). Phytoplankton of the western Arctic in the spring and summer of 2002: Structure and seasonal changes. *Deep Sea Res. Part II: Topical Stud. Oceanography* 56, 1223–1236. doi: 10.1016/j.dsr2.2008.12.030
- Tillmann, U., Jaén, D., Fernández, L., Gottschling, M., Witt, M., Blanco, J., et al. (2017). *Amphidoma languida* (Amphidomatacea, Dinophyceae) with a novel azaspiracid toxin profile identified as the cause of molluscan contamination at the Atlantic coast of southern Spain. *Harmful Algae* 62, 113–126. doi: 10.1016/j.hal.2016.12.001
- Tillmann, U., Kremp, A., Tahvanainen, P., and Krock, B. (2014). Characterization of spirolide producing *Alexandrium ostenfeldii* (Dinophyceae) from the western Arctic. *Harmful Algae* 39, 259–270. doi: 10.1016/j.hal.2014.08.008
- Tillmann, U., Krock, B., Alpermann, T. J., and Cembella, A. (2016). Bioactive compounds of marine dinoflagellate isolates from western Greenland and their

phylogenetic association within the genus *Alexandrium*. *Harmful Algae* 51, 67–80. doi: 10.1016/j.hal.2015.11.004

Tillmann, U., Wietkamp, S., Krock, B., Tillmann, A., Voss, D., and Gu, H. (2020). Amphidomataceae (Dinophyceae) in the western Greenland area, including description of *Azadinium perforatum* sp. nov. *Phycologia* 59, 63–88. doi: 10.1080/00318884.2019.1670013

Toebe, K., Alpermann, T. J., Tillmann, U., Krock, B., Cembella, A., and John, U. (2013). Molecular discrimination of toxic and non-toxic *Alexandrium* species (Dinophyta) in natural phytoplankton assemblages from the Scottish coast of the North Sea. *Eur. J. Phycol* 48, 12–26. doi: 10.1080/09670262.2012.752870

Touzet, N., Franco, J. M., and Raine, R. (2008). PSP toxin analysis and discrimination of the naturally co-occurring *Alexandrium tamarense* and *A. minutum* (Dinophyceae) in Cork Harbour, Ireland. *Aquat. Microbial Ecol.* 51, 285–299. doi: 10.3354/ame01189

Van de Waal, D. B., Tillmann, U., Martens, H., Krock, B., van Scheppingen, Y., and John, U. (2015). Characterization of multiple isolates from an *Alexandrium ostenfeldii* bloom in The Netherlands. *Harmful Algae* 49, 94–104. doi: 10.1016/j.hal.2015.08.002

Verity, P. G., Brussaard, C. P., Nejtgaard, J. C., van Leeuwe, M. A., Lancelot, C., and Medlin, L. K. (2007). Current understanding of *Phaeocystis* ecology and biogeochemistry, and perspectives for future research. *Biogeochemistry* 83, 311–330. doi: 10.1007/s10533-007-9090-6

Wassmann, P. (2011). Arctic marine ecosystems in an era of rapid climate change. *Prog. Oceanogr* 90, 1–17. doi: 10.1016/j.pocan.2011.02.002

Wietz, M., Bienhold, C., Metfies, K., Torres-Valdés, S., von Appen, W. J., Salter, I., et al. (2021). The polar night shift: seasonal dynamics and drivers of Arctic Ocean microbiomes revealed by autonomous sampling. *ISME Commun.* 1, 76. doi: 10.1038/s43705-021-00074-4